Fractional action cosmology: some dark energy models in emergent, logamediate, and intermediate scenarios of the universe

Ujjal Debnath[1]
Email: ujjaldebnath@yahoo.com

Surajit Chattopadhyay[2*]
*Corresponding author
Email: surajit_2008@yahoo.co.in

Mubasher Jamil[3,4]
Email: mjamil@camp.nust.edu.pk

[1]Department of Mathematics, Bengal Engineering and Science University, Shibpur, Howrah, 711-103, India

[2]Pailan College of Management and Technology, Bengal Pailan Park, Kolkata, 700-104, India

[3]Center for Advanced Mathematics and Physics (CAMP), National University of Sciences and Technology (NUST), H-12, Islamabad, Pakistan

[4]Eurasian International Center for Theoretical Physics, Eurasian National University, Astana, 010008, Kazakhstan

Archive of SID

Abstract

In the framework of fractional action cosmology, we have reconstructed the scalar potentials and scalar fields, namely, quintessence, phantom, tachyon, k-essence, Dirac-Born-Infeld-essence, hessence, dilaton field, and Yang-Mills field. To get more physical picture of the variation of the scalar field and potential with time, we express a scale factor in emergent, logamediate, and intermediate scenarios, under which the universe expands differently.

Keywords

Dark energy, Fractional action cosmology, Emergent, Logamediate, Intermediate, Universe

PACS

98.80.Cq, 95.36.+x

Background

Fractional action cosmology (FAC) is based on the principles and formalism of the fractional calculus applied to cosmology. The fractional derivative and fractional integrals are the main tools in fractional calculus, where the order of differentiation or integration is not an integer. The fractional calculus is

www.SID.ir

immensely useful in various branches of mathematics, physics, and engineering [1]. In doing FAC, one can proceed in two different ways [2,3]: the first one is quite easy as one has to replace the partial derivatives in the Einstein field equations with the corresponding fractional derivatives [2]; the second technique involves deriving the field equations and geodesic equations from a more fundamental way, namely starting with the principle of least action and replacing the usual integral with a fractional integral. In the framework of FAC, the gravitational field is represented by an affine connection on a curved manifold, and the free fall for a particle of mass m corresponds to a geodesic motion with an action given by [4,5]:

$$S = -\frac{m}{2\Gamma(\xi)} \int \dot{x}^{\mu}\dot{x}^{\nu} g_{\mu\nu}(x)(t-\tau)^{\xi-1} d\tau. \tag{1a}$$

Here $\Gamma(\xi) = \int_0^{\infty} t^{\xi-1}e^{-t}dt$ is the gamma function, $0 < \xi \leq 1$, $0 < \tau < t$, m = constant, and $\dot{x}^{\mu} = \frac{dx^{\mu}}{d\tau}$. The $g_{\mu\nu}$ is the metric tensor. The variation yields an extra term in the field equations which he termed as 'variable gravitational constant G'. Moreover, when the weight function in the fractional time integral is replaced with a sinusoidal function, then the solution of the corresponding field equations yields a variable cosmological constant and an oscillatory scale factor [6]:

$$S = \frac{m}{2} \int_0^{\tau} \dot{x}^{\mu}\dot{x}^{\nu} g_{\mu\nu}(x) e^{-\chi \sin(\beta t)} dt, \tag{1b}$$

where $\chi = 0$ reduces to the standard action. In [7], the authors extended the previous study by working out with a general weight function:

$$S = \frac{m}{2} \int_0^{\tau} g_{\mu\nu}(x)\dot{x}^{\mu}\dot{x}^{\nu}\mu(\chi, t) dt. \tag{1c}$$

Several examples were studied, and cosmological parameters were calculated in there. An interesting feature of FAC is that it yields an expanding universe, the scale factor of which goes like a power law form or exponential form depending on the choice of the weight function. Hence, cosmic acceleration can be modeled in FAC. It should also be mentioned that FAC modeled not only late acceleration but also graviton field [4].

Reconstruction of potentials has been done by several authors in various cases [8-16]. Also, various scenarios of the universe have been considered in the works of [17-22]. Capozziello et al. [23] considered scalar-tensor theories and reconstruct their potential and coupling by demanding a background ΛCDM cosmology. In the framework of phantom quintessence cosmology, [24] used the Noether symmetry approach to obtain general exact solutions for the cosmological equations. In the present paper, we are going to reconstruct the potentials and scalar fields, namely, quintessence, phantom, tachyonic, k-essence, Dirac-Born-Infeld (DBI)-essence, hessence, dilaton field, and Yang-Mills field. Such reconstructions have been studied previously in other gravitational setups [8-16]. To get more physical insight into the model, we express scale factor in three useful forms [17-22] (emergent, logamediate, and intermediate scenarios) under which the universe expands differently. Such expansion scenarios are consistent with the observations with some restrictions on their parameters [17-22].

Fractional action cosmological model

For a Friedmann-Robertson-Walker (FRW) spacetime, the line element is

$$ds^2 = -dt^2 + a^2(t)\left[\frac{dr^2}{1-kr^2} + r^2(d\theta^2 + \sin^2\theta d\phi^2)\right], \tag{2}$$

Archive of SID

www.SID.ir

where $a(t)$ is the scale factor, and k $(= 0, \pm 1)$ is the curvature scalar. We consider that the universe contains normal matter and dark energy. From Equation (1a), the Einstein equations for the space-time given by Equation (2) are [4,5]

$$H^2 + \frac{2(\xi-1)}{T_1}H + \frac{k}{a^2} = \frac{8\pi G}{3}\rho, \tag{3}$$

$$\dot{H} - \frac{(\xi-1)}{T_1}H - \frac{k}{a^2} = -4\pi G(\rho + p), \tag{4}$$

where $T_1 = t - \tau$, $\rho = (\rho_{\rm m} + \rho_\phi)$, and $p = (p_{\rm m} + p_\phi)$. Here, $\rho_{\rm m}$ and $p_{\rm m}$ are the energy density and pressure of the normal matter connected by the equation of state (EoS)

$$p_{\rm m} = w_m \rho_{\rm m}\ , \quad -1 \leq w_m \leq 1, \tag{5}$$

and ρ_ϕ and p_ϕ are the energy density and pressure due to the dark energy, respectively.

Now, consider there is an interaction between normal matter and dark energy. Dark energy interacting with dark matter is a promising model to alleviate the cosmic coincidence problem. In [25], the authors studied the signature of such interaction on large scale cosmic microwave background (CMB) temperature anisotropies. Based on the detailed analysis on perturbation equations of dark energy and dark matter when they are in interaction, they found that the large scale CMB, especially the late integrated Sachs Wolfe effect, is a useful tool to measure the coupling between dark sectors. It was deduced that in the 1σ range, the constrained coupling between dark sectors can solve the coincidence problem. In [26], a general formalism to study the growth of dark matter perturbations when dark energy perturbates and interacts between the dark sectors were presented.

They showed that the dynamical stability on the growth of structure depends on the form of coupling between dark sectors. Moreover, due to the influence of the interaction, the growth index can differ from the value without interaction by an amount up to the observational sensibility, which provides an opportunity to probe the interaction between dark sectors through future observations on the growth of the structure.

Due to this interaction, the normal matter and dark energy are not separately conserved. The energy conservation equations for normal matter and dark energy are

$$\dot{\rho}_m + 3H(p_m + \rho_m) = -3\delta H \rho_m, \tag{6}$$

and

$$\dot{\rho}_\phi + 3H(p_\phi + \rho_\phi) = 3\delta H \rho_m, \tag{7}$$

respectively, where $H = \dot{a}/a$ is the Hubble parameter.

From Equation (6), we have the expression for energy density of matter as

$$\rho_m = \rho_0 a^{-3(1+w_m+\delta)}, \tag{8}$$

where ρ_0 is the integration constant.

Emergent, logamediate, and intermediate scenarios

- Emergent scenario: For emergent universe, the scale factor can be chosen as [27,28]

$$a(T_1) = a_0 \left(\lambda + e^{\mu T_1}\right)^n, \tag{9}$$

Archive of SID

www.SID.ir

where a_0, μ, λ, and n are positive constants. (1) $a_0 > 0$ for the scale factor a to be positive; (2) $\lambda > 0$, to avoid any singularity at finite time (big rip); (3) $a > 0$ or $n > 0$ for expanding model of the universe; (4) $a < 0$ and $n < 0$ imply big bang singularity at $t = -\infty$.

So, the Hubble parameter and its derivatives are given by

$$H = \frac{n\mu e^{\mu T_1}}{(\lambda + e^{\mu T_1})}\ ,\ \dot{H} = \frac{n\lambda\mu^2 e^{\mu T_1}}{(\lambda + e^{\mu T_1})^2}\ ,\ \ddot{H} = \frac{n\lambda\mu^3 e^{\mu T_1}(\lambda - e^{\mu T_1})}{(\lambda + e^{\mu T_1})^3}. \tag{10}$$

Here, H and $\dot{H}$ are both positive, but $\ddot{H}$ changes sign at $T_1 = \frac{1}{\mu}\log\lambda$. Thus H, $\dot{H}$, and $\ddot{H}$ all tend to zero as $t \to -\infty$. On the other hand, as $t \to \infty$, the solution gives asymptotically a de Sitter universe.

- Logamediate scenario: Consider a particular form of logamediate scenario, where the form of the scale factor $a(t)$ is defined as [17-22]

$$a(T_1) = e^{A(\ln T_1)^\alpha}, \tag{11}$$

where $A\alpha > 0$ and $\alpha > 1$. When $\alpha = 1$, this model reduces to a power law form. The logamediate form is motivated by considering a class of possible cosmological solutions with indefinite expansion which results from imposing weak general conditions on the cosmological model. Barrow and others [17-22] have found that, in their model, the observational ranges of the parameters are as follows: $1.5 \times 10^{-92} \leq A \leq 2.1 \times 10^{-2}$ and $2 \leq \alpha \leq 50$. The Hubble parameter $H = \frac{\dot{a}}{a}$ and its derivative become

$$H = \frac{A\alpha}{T_1}(\ln T_1)^{\alpha-1}\ \ ,\ \ \dot{H} = \frac{A\alpha}{T_1^2}(\ln T_1)^{\alpha-2}(\alpha - 1 - \ln T_1). \tag{12}$$

- Intermediate scenario: Consider a particular form of intermediate scenario, where the scale factor $a(t)$ of the Friedmann universe is described as [17-22]

$$a(t) = e^{BT_1^\beta}, \tag{13}$$

where $B\beta > 0$, $B > 0$, and $0 < \beta < 1$. Here, the expansion of universe is faster than the power law form, where the scale factor is given as $a(T_1) = T_1^n$ (where $n > 1$ is a constant). Also, the expansion of the universe is slower for standard de Sitter scenario, where $\beta = 1$. The Hubble parameter $H = \frac{\dot{a}}{a}$ and its derivative become

$$H = B\beta T_1^{\beta-1}\ ,\ \ \dot{H} = B\beta(\beta - 1)T_1^{\beta-2}. \tag{14}$$

Various candidates of dark energy models

Quintessence or phantom field

Quintessence is described by an ordinary time-dependent and homogeneous scalar field ϕ which is minimally coupled to gravity but with a particular potential $V(\phi)$ that leads to the accelerating universe. The action for quintessence is given by [29]

$$S = \int \mathrm{d}^4x\sqrt{-g}\left[-\frac{1}{2}g^{ij}\partial_i\phi\partial_j\phi - V(\phi)\right].$$

Archive of SID

www.SID.ir

The energy momentum tensor of the field is

$$T_{ij} = -\frac{2}{\sqrt{-g}}\frac{\delta S}{\delta g^{ij}},$$

which gives

$$T_{ij} = \partial_i\phi\partial_j\phi - g_{ij}\left[\frac{1}{2}g^{kl}\partial_k\phi\partial_l\phi + V(\phi)\right].$$

The energy density and pressure of the quintessence scalar field ϕ are as follows:

$$\rho_\phi = -T_0^0 = \frac{1}{2}\dot{\phi}^2 + V(\phi),$$

$$p_\phi = T_i^i = \frac{1}{2}\dot{\phi}^2 - V(\phi).$$

The EoS parameter for the quintessence scalar field is given by

$$\omega_\phi = \frac{p_\phi}{\rho_\phi} = \frac{\dot{\phi}^2 - 2V(\phi)}{\dot{\phi}^2 + 2V(\phi)}.$$

For $\omega_\phi < -1/3$, we find that the universe accelerates when $\dot{\phi}^2 < V(\phi)$. The energy density and the pressure of the quintessence (phantom field) can be represented by the minimally coupled spatially homogeneous and time-dependent scalar field ϕ having positive (negative) kinetic energy term given by

$$\rho_\phi = \frac{\epsilon}{2}\dot{\phi}^2 + V(\phi) \tag{15}$$

and

$$p_\phi = \frac{\epsilon}{2}\dot{\phi}^2 - V(\phi), \tag{16}$$

where $V(\phi)$ is the relevant potential for the scalar field ϕ; $\epsilon = +1$ represents quintessence, while $\epsilon = -1$ refers to phantom field.

Scalar field models of phantom energy indicate that it can behave as a long range repulsive force [30]. Moreover, the phantom energy has few characteristics different from normal matter, for instance, the energy density $\rho(t)$ of the phantom field increases with the expansion of the universe. It can be used as a source to form and stabilize traversable wormholes [31-35]. The phantom energy can disrupt all gravitationally bound structures, i.e, from galaxies to black holes [36-41]. It can produce infinite expansion of the universe in a finite time, thus causing the 'big rip' [42,43]. In Equations (3) and (4), we put the forms of p_ϕ and ρ_ϕ expressed above. The Hubble parameter (H) is obtained based on the form of the scale factor. First, we separate the scalar field and potential as follows:

$$\dot{\phi}^2 = -\frac{(1+w_m)}{\epsilon}\rho_m + \frac{1}{4\pi\epsilon G}\left[-\dot{H} + \frac{(\xi-1)}{T_1}H + \frac{k}{a^2}\right], \tag{17}$$

and

$$V = \frac{(w_m-1)}{2}\rho_m + \frac{1}{8\pi G}\left[\dot{H} + 3H^2 + \frac{5(\xi-1)}{T_1}H + \frac{2k}{a^2}.\right] \tag{18}$$

Similar approach would be adopted for other scalar field models of dark energy. Now, we consider the various choices of scale factor:

Archive of SID

www.SID.ir

- For emergent scenario, we get the expressions for ϕ and V as

$$\phi = \int \sqrt{-\frac{(1+w_m)\rho_0 a_0^{-3(1+w_m+\delta)}}{\epsilon\,(\lambda+e^{\mu T_1})^{3n(1+w_m+\delta)}} + \frac{1}{4\pi\epsilon G}\left\{-\frac{n\lambda\mu^2 e^{\mu T_1}}{(\lambda+e^{\mu T_1})^2} + \frac{(\xi-1)n\mu e^{\mu T_1}}{T_1(\lambda+e^{\mu T_1})} + \frac{k\,a_0^{-2}}{(\lambda+e^{\mu T_1})^{2n}}\right\}}\; dT_1, \tag{19}$$

and

$$V = \frac{(w_m-1)\rho_0 a_0^{-3(1+w_m+\delta)}}{2\,(\lambda+e^{\mu T_1})^{3n(1+w_m+\delta)}} + \frac{1}{8\pi G}\left\{\frac{n\mu^2 e^{\mu T_1}(\lambda+3ne^{\mu T_1})}{(\lambda+e^{\mu T_1})^2} + \frac{5(\xi-1)n\mu e^{\mu T_1}}{T_1(\lambda+e^{\mu T_1})} + \frac{2k\,a_0^{-2}}{(\lambda+e^{\mu T_1})^{2n}}\right\}. \tag{20}$$

- For logamediate scenario, we get the expressions for ϕ and V as

$$\phi = \int \sqrt{-\frac{(1+w_m)\rho_0}{\epsilon}\, e^{-3A(1+w_m+\delta)(\ln T_1)^\alpha} + \frac{1}{4\pi\epsilon G}\left\{\frac{A\alpha}{T_1^2}(\ln T_1)^{\alpha-2}(1-\alpha+\xi\ln T_1) + k\, e^{-2A(\ln T_1)^\alpha}\right\}}\; dT_1 \tag{21}$$

and

$$V = \frac{(w_m-1)\rho_0}{2}\, e^{-3A(1+w_m+\delta)(\ln T_1)^\alpha} + \frac{1}{8\pi G}\left[\frac{A\alpha}{T_1^2}(\ln T_1)^{\alpha-2}\{\alpha-1+(5\xi-6)\ln T_1 + 3A\alpha(\ln T_1)^\alpha\} + 2k\, e^{-2A(\ln T_1)^\alpha}\right]. \tag{22}$$

- For intermediate scenario, we get the expressions for ϕ and V as

$$\phi = \int \sqrt{-\frac{(1+w_m)\rho_0}{\epsilon}\, e^{-3B(1+w_m+\delta)T_1^\beta} + \frac{1}{4\pi\epsilon G}\left\{B\beta(\xi-\beta)T_1^{\beta-2} + k\, e^{-2BT_1^\beta}\right\}}\; dT_1, \tag{23}$$

and

$$V = \frac{(w_m-1)\rho_0}{2}\, e^{-3B(1+w_m+\delta)T_1^\beta} + \frac{1}{8\pi G}\left[B\beta T_1^{\beta-2}(5\xi+\beta+3B\beta T_1^\beta) + 2k\, e^{-2BT_1^\beta}\right]. \tag{24}$$

In Figures 1, 2, and 3, we have plotted the potentials versus the scalar fields for the quintessence and phantom fields in emergent, logamediate, and intermediate scenarios of the universe, respectively, in fractional action cosmology. It has been observed in Figure 1 that after gradual decay, the potential starts increasing with scalar field for quintessence as well as phantom field models of dark energy in the emergent scenario of the universe irrespective of its type of curvature. On the contrary, when logamediate scenario is considered, the Figure 2 exhibits a continuous decay in the potential V with increase in the scalar field ϕ. A different behavior is observed in Figure 3 that depicts the behavior of the potential V versus scalar field ϕ in the case of intermediate scenario of the universe. The blue lines in this figure show a continuous decay in V with increase in ϕ for quintessence model. However, the red lines exhibit an increasing pattern of V with scalar field ϕ.

Figure 1 Variations of V against quintessence or phantom field ϕ in the emergent scenario. Solid, dash, and dotted lines represent $k=-1$, $k=+1$, and $k=0$, respectively. Blue and red lines represent quintessence field ($\epsilon=+1$) and phantom field ($\epsilon=-1$), respectively.

Figure 2 Variations of V against quintessence or phantom field ϕ in the logamediate scenario. Solid, dash, and dotted lines represent $k=-1$, $k=+1$, and $k=0$, respectively. Blue and red lines represent quintessence field ($\epsilon=+1$) and phantom field ($\epsilon=-1$), respectively.

Archive of SID

www.SID.ir

Figure 3 Variations of V against quintessence or phantom field ϕ in the intermediate scenario. Solid, dash, and dotted lines represent $k = -1$,$k = +1$, and $k = 0$, respectively. Blue and red lines represent quintessence field ($\epsilon = +1$) and phantom field ($\epsilon = -1$), respectively.

Tachyonic field

A rolling tachyon has an interesting equation of state, the state parameter of which smoothly interpolates between -1 and 0 [44]. Thus, tachyon can be realized as a suitable candidate for the inflation at high energy [45-47] as well as a source of dark energy, depending on the form of the tachyon potential [48-51]. Therefore, it becomes meaningful to reconstruct tachyon potential $V(\phi)$ from some dark energy models. An action for tachyon scalar ϕ is given by Born-Infeld-like action

$$S = -\int d^4x\sqrt{-g}V(\phi)\sqrt{1 - g^{ij}\partial_i\phi\partial_j\phi}, \tag{25}$$

where $V(\phi)$ is the tachyon potential. Energy-momentum tensor components for tachyon scalar ϕ are obtained as

$$T_{ij} = V(\phi)\left[\frac{\partial_i\phi\partial_j\phi}{\sqrt{1 - g^{ij}\partial_i\phi\partial_j\phi}} + g_{ij}\sqrt{1 - g^{kl}\partial_k\phi\partial_l\phi}\right]. \tag{26}$$

The energy density ρ_ϕ and pressure p_ϕ due to the tachyonic field ϕ have the expressions

$$\rho_\phi = \frac{V(\phi)}{\sqrt{1 - \epsilon\dot{\phi}^2}}, \tag{27}$$

$$p_\phi = -V(\phi)\sqrt{1 - \epsilon\dot{\phi}^2}, \tag{28}$$

where $V(\phi)$ is the relevant potential for the tachyonic field ϕ. It is to be seen that $\frac{p_\phi}{\rho_\phi} = -1 + \epsilon\dot{\phi}^2 > -1$ or < -1 accordingly as normal tachyon ($\epsilon = +1$) or phantom tachyon ($\epsilon = -1$).

From above, we get

$$\dot{\phi}^2 = \left[-\frac{(1 + w_m)}{\epsilon}\rho_m + \frac{1}{4\pi\epsilon G}\left\{-\dot{H} + \frac{(\xi - 1)}{T_1}H + \frac{k}{a^2}\right\}\right] \times \left[-\rho_m + \frac{3}{8\pi G}\left\{H^2 + \frac{2(\xi - 1)}{T_1}H + \frac{k}{a^2}\right\}\right]^{-1} \tag{29}$$

and

$$V = \left[w_m\rho_m + \frac{1}{8\pi G}\left\{2\dot{H} + 3H^2 + \frac{4(\xi - 1)}{T_1}H + \frac{k}{a^2}\right\}\right]^{\frac{1}{2}} \times \left[-\rho_m + \frac{3}{8\pi G}\left\{H^2 + \frac{2(\xi - 1)}{T_1}H + \frac{k}{a^2}\right\}\right]^{\frac{1}{2}}. \tag{30}$$

Archive of SID

www.SID.ir

- For emergent scenario, we get the expressions for ϕ and V as

$$\phi = \int \left[-\frac{(1+w_m)\rho_0 a_0^{-3(1+w_m+\delta)}}{\epsilon\left(\lambda+e^{\mu T_1}\right)^{3n(1+w_m+\delta)}} + \frac{1}{4\pi\epsilon G}\left\{ -\frac{n\lambda\mu^2 e^{\mu T_1}}{\left(\lambda+e^{\mu T_1}\right)^2} + \frac{(\xi-1)n\mu e^{\mu T_1}}{T_1(\lambda+e^{\mu T_1})} + \frac{k\, a_0^{-2}}{\left(\lambda+e^{\mu T_1}\right)^{2n}} \right\} \right]^{\frac{1}{2}}$$

$$\times \left[-\frac{\rho_0 a_0^{-3(1+w_m+\delta)}}{\left(\lambda+e^{\mu T_1}\right)^{3n(1+w_m+\delta)}} + \frac{3}{8\pi G}\left\{ \frac{n^2\mu^2 e^{2\mu T_1}}{\left(\lambda+e^{\mu T_1}\right)^2} + \frac{2(\xi-1)n\mu e^{\mu t}}{T_1(\lambda+e^{\mu T_1})} + \frac{k\, a_0^{-2}}{\left(\lambda+e^{\mu T_1}\right)^{2n}} \right\} \right]^{-\frac{1}{2}} dT_1 \tag{31}$$

and

$$V = \left[\frac{w_m\rho_0 a_0^{-3(1+w_m+\delta)}}{\left(\lambda+e^{\mu T_1}\right)^{3n(1+w_m+\delta)}} + \frac{1}{8\pi G}\left\{ \frac{n\mu^2 e^{\mu T_1}(2\lambda+3ne^{\mu T_1})}{\left(\lambda+e^{\mu T_1}\right)^2} + \frac{4(\xi-1)n\mu e^{\mu T_1}}{T_1(\lambda+e^{\mu T_1})} + \frac{k\, a_0^{-2}}{\left(\lambda+e^{\mu T_1}\right)^{2n}} \right\} \right]^{\frac{1}{2}}$$

$$\times \left[-\frac{\rho_0 a_0^{-3(1+w_m+\delta)}}{\left(\lambda+e^{\mu T_1}\right)^{3n(1+w_m+\delta)}} + \frac{3}{8\pi G}\left\{ \frac{n^2\mu^2 e^{2\mu T_1}}{\left(\lambda+e^{\mu T_1}\right)^2} + \frac{2(\xi-1)n\mu e^{\mu T_1}}{T_1(\lambda+e^{\mu T_1})} + \frac{k\, a_0^{-2}}{\left(\lambda+e^{\mu T_1}\right)^{2n}} \right\} \right]^{\frac{1}{2}}. \tag{32}$$

- For logamediate scenario, we get the expressions for ϕ and V as

$$\phi = \int \left[-\frac{(1+w_m)\rho_0}{\epsilon}\, e^{-3A(1+w_m+\delta)(\ln T_1)^\alpha} + \frac{1}{4\pi\epsilon G}\left\{ \frac{A\alpha}{T_1^2}(\ln T_1)^{\alpha-2}(1-\alpha+\xi\ln T_1) + k\, e^{-2A(\ln T_1)^\alpha} \right\} \right]^{\frac{1}{2}}$$

$$\times \left[-\rho_0\, e^{-3A(1+w_m+\delta)(\ln T_1)^\alpha} + \frac{3}{8\pi G}\left\{ \frac{A\alpha}{T_1^2}(\ln T_1)^{\alpha-1}\{A\alpha(\ln T_1)^{\alpha-1}+2(\xi-1)\} + k\, e^{-2A(\ln T_1)^\alpha} \right\} \right]^{-\frac{1}{2}} dT_1 \tag{33}$$

and

$$V = \left[-\rho_0\, e^{-3A(1+w_m+\delta)(\ln T_1)^\alpha} + \frac{3}{8\pi G}\left\{ \frac{A\alpha}{T_1^2}(\ln T_1)^{\alpha-1}\{A\alpha(\ln T_1)^{\alpha-1}+2(\xi-1)\} + k\, e^{-2A(\ln T_1)^\alpha} \right\} \right]^{\frac{1}{2}}$$

$$\times \left[w_m\rho_0\, e^{-3A(1+w_m+\delta)(\ln T_1)^\alpha} + \frac{1}{8\pi G}\left\{ \frac{A\alpha}{t^2}(\ln T_1)^{\alpha-2}\{2(\alpha-1)+2(\xi-3)\ln t + 3A\alpha(\ln T_1)^\alpha\} + k\, e^{-2A(\ln T_1)^\alpha} \right\} \right]^{\frac{1}{2}}. \tag{34}$$

- For intermediate scenario, we get the expressions for ϕ and V as

$$\phi = \int \left[-\frac{(1+w_m)\rho_0}{\epsilon}\, e^{-3B(1+w_m+\delta)T_1^\beta} + \frac{1}{4\pi\epsilon G}\left\{ B\beta(\xi-\beta)T_1^{\beta-2} + k\, e^{-2BT_1^\beta} \right\} \right]^{\frac{1}{2}}$$

$$\times \left[-\rho_0\, e^{-3B(1+w_m+\delta)T_1^\beta} + \frac{3}{8\pi G}\left\{ B\beta T_1^{\beta-2}(2(\xi-1)+B\beta T_1^\beta) + k\, e^{-2BT_1^\beta} \right\} \right]^{-\frac{1}{2}} dT_1 \tag{35}$$

and

$$V = \left[-\rho_0\, e^{-3B(1+w_m+\delta)T_1^\beta} + \frac{3}{8\pi G}\left\{ B\beta T_1^{\beta-2}(2(\xi-1)+B\beta T_1^\beta) + k\, e^{-2BT_1^\beta} \right\} \right]^{\frac{1}{2}}$$

$$\times \left[w_m\rho_0\, e^{-3B(1+w_m+\delta)T_1^\beta} + \frac{1}{8\pi G}\left\{ B\beta T_1^{\beta-2}(2(2\xi+\beta-3)+3B\beta T_1^\beta) + k\, e^{-2BT_1^\beta} \right\} \right]^{\frac{1}{2}}. \tag{36}$$

Archive of SID

www.SID.ir

In Figure 4, the V-ϕ plot for normal tachyon and phantom tachyon models of dark energy is presented for emergent scenario of the universe. The potential of normal tachyon exhibits decaying pattern. However, it shows an increasing pattern for phantom tachyonic field ϕ. It happens irrespective of the curvature of the universe. In the logamediate scenario (Figure 5) the potentials for normal tachyon and phantom tachyon exhibit increasing and decreasing behavior, respectively, with the increase in the scalar field ϕ. From Figure 6, we see a continuous decay in the potential for normal tachyonic field in the intermediate scenario. However, in this scenario, the behavior of the potential varies with the curvature of the universe characterized by interacting phantom tachyonic field. For $k = -1$ and $k = 1$, the potential increases with phantom tachyonic field; for $k = 0$, it decays after increasing initially.

Figure 4 Variations of V against tachyonic field ϕ in the emergent scenario. Solid, dash, and dotted lines represent $k = -1$, $k = +1$, and $k = 0$, respectively. Blue and red lines represent normal tachyonic field ($\epsilon = +1$) and phantom tachyonic field ($\epsilon = -1$), respectively.

Figure 5 Variations of V against tachyonic field ϕ in the logamediate scenario. Solid, dash, and dotted lines represent $k = -1$, $k = +1$, and $k = 0$, respectively. Blue and red lines represent normal tachyonic field ($\epsilon = +1$) and phantom tachyonic field ($\epsilon = -1$), respectively.

Figure 6 Variations of V against tachyonic field ϕ in the intermediate scenario. Solid, dash, and dotted lines represent $k = -1$, $k = +1$, and $k = 0$, respectively. Blue and red lines represent normal tachyonic field ($\epsilon = +1$) and phantom tachyonic field ($\epsilon = -1$), respectively.

---

k-essence

In the kinetically driven scalar field theory, we have *non-canonical* kinetic energy term with *no* potential. Scalars modelling this theory are popularly known as *k-essence*. Motivated by Born-Infeld action of String Theory, it was used as a source to explain the mechanism for producing the late time acceleration of the universe. This model is given by the action [52-57]

$$S = \int d^4x\sqrt{-g}\tilde{\mathcal{L}}(\tilde{\phi}, \tilde{X}), \tag{37}$$

with

$$\tilde{\mathcal{L}}(\tilde{\phi}, \tilde{X}) = K(\tilde{\phi})\tilde{X} + L(\tilde{\phi})\tilde{X}^2, \tag{38}$$

ignoring the higher order terms of

$$\tilde{X} = \frac{1}{2}g^{ij}\partial_i\tilde{\phi}\partial_j\tilde{\phi}. \tag{39}$$

Using the following transformations, $\phi = \int d\tilde{\phi}\sqrt{|L(\tilde{\phi})|/K(\tilde{\phi})}$, $X = \frac{|L|}{K}\tilde{X}$, and $V(\phi) = K^2/|L|$, the action can be rewritten as

$$S = \int d^4x\sqrt{-g}V(\phi)\mathcal{L}(X), \tag{40}$$

with

$$\mathcal{L}(X) = X - X^2. \tag{41}$$

From the action, the energy-momentum tensor components can be written as

$$T_{ij} = V(\phi)\left[\frac{d\mathcal{L}}{dX}\partial_i\phi\partial_j\phi - g_{ij}\mathcal{L}\right]. \tag{42}$$

Archive of SID

www.SID.ir

The energy density and pressure of k-essence scalar field ϕ are given by

$$\rho_{\rm k} = V(\phi)(-X + 3X^2) \tag{43}$$

and

$$p_{\rm k} = V(\phi)(-X + X^2), \tag{44}$$

where ϕ is the scalar field having a kinetic energy $X = \frac{1}{2}\dot{\phi}^2$, and $V(\phi)$ is the k-essence potential.

From above, we get

$$\dot{\phi}^2 = \left[2(w_m-1)\rho_m + \frac{1}{2\pi G}\left\{\dot{H} + 3H^2 + \frac{5(\xi-1)}{T_1}H + \frac{2k}{a^2}\right\}\right] \times \left[(3w_m-1)\rho_m + \frac{3}{4\pi G}\left\{\dot{H} + 2H^2 + \frac{3(\xi-1)}{T_1}H + \frac{k}{a^2}\right\}\right]^{-1}, \tag{45}$$

and

$$V = \left[(3w_m-1)\rho_m + \frac{3}{4\pi G}\left\{\dot{H} + 2H^2 + \frac{3(\xi-1)}{T_1}H + \frac{k}{a^2}\right\}\right]^2 \times \left[2(w_m-1)\rho_m + \frac{1}{2\pi G}\left\{\dot{H} + 3H^2 + \frac{5(\xi-1)}{T_1}H + \frac{2k}{a^2}\right\}\right]^{-1}. \tag{46}$$

- For emergent scenario, we have

$$\phi = \int \left[\frac{2(w_m-1)\rho_0 a_0^{-3(1+w_m+\delta)}}{(\lambda+e^{\mu T_1})^{3n(1+w_m+\delta)}} + \frac{1}{2\pi G}\left\{\frac{n\mu^2 e^{\mu T_1}(\lambda+3ne^{\mu T_1})}{(\lambda+e^{\mu T_1})^2} + \frac{5(\xi-1)n\mu e^{\mu T_1}}{T_1(\lambda+e^{\mu T_1})} + \frac{2k\,a_0^{-2}}{(\lambda+e^{\mu T_1})^{2n}}\right\}\right]^{\frac{1}{2}} \times \left[\frac{(3w_m-1)\rho_0 a_0^{-3(1+w_m+\delta)}}{(\lambda+e^{\mu T_1})^{3n(1+w_m+\delta)}} + \frac{3}{4\pi G}\left\{\frac{n\mu^2 e^{\mu T_1}(\lambda+2ne^{\mu T_1})}{(\lambda+e^{\mu T_1})^2} + \frac{3(\xi-1)n\mu e^{\mu T_1}}{T_1(\lambda+e^{\mu T_1})} + \frac{k\,a_0^{-2}}{(\lambda+e^{\mu T_1})^{2n}}\right\}\right]^{-\frac{1}{2}} dt, \tag{47}$$

and

$$V = \left[\frac{(3w_m-1)\rho_0 a_0^{-3(1+w_m+\delta)}}{(\lambda+e^{\mu T_1})^{3n(1+w_m+\delta)}} + \frac{3}{4\pi G}\left\{\frac{n\mu^2 e^{\mu T_1}(\lambda+2ne^{\mu T_1})}{(\lambda+e^{\mu T_1})^2} + \frac{3(\xi-1)n\mu e^{\mu T_1}}{T_1(\lambda+e^{\mu T_1})} + \frac{k\,a_0^{-2}}{(\lambda+e^{\mu T_1})^{2n}}\right\}\right]^2 \times \left[\frac{2(w_m-1)\rho_0 a_0^{-3(1+w_m+\delta)}}{(\lambda+e^{\mu T_1})^{3n(1+w_m+\delta)}} + \frac{1}{2\pi G}\left\{\frac{n\mu^2 e^{\mu T_1}(\lambda+3ne^{\mu T_1})}{(\lambda+e^{\mu T_1})^2} + \frac{5(\xi-1)n\mu e^{\mu T_1}}{T_1(\lambda+e^{\mu T_1})} + \frac{2k\,a_0^{-2}}{(\lambda+e^{\mu T_1})^{2n}}\right\}\right]^{-1}. \tag{48}$$

- For logamediate scenario, we get the expressions for ϕ and V as

$$\phi = \int \left[2(w_m-1)\rho_0\, e^{-3A(1+w_m+\delta)(\ln T_1)^\alpha} + \frac{1}{2\pi G}\left\{\frac{A\alpha}{T_1^2}(\ln T_1)^{\alpha-2}(\alpha-1+(5\xi-6)\ln T_1 + 3A\alpha(\ln T_1)^\alpha) + 2k\, e^{-2A(\ln T_1)^\alpha}\right\}\right]^{\frac{1}{2}} \times \left[(3w_m-1)\rho_0\, e^{-3A(1+w_m+\delta)(\ln T_1)^\alpha} + \frac{3}{4\pi G}\left\{\frac{A\alpha}{T_1^2}(\ln T_1)^{\alpha-2}(\alpha-1+(3\xi-4)\ln T_1 + 2A\alpha(\ln T_1)^\alpha) + k\, e^{-2A(\ln T_1)^\alpha}\right\}\right]^{-\frac{1}{2}} dT_1, \tag{49}$$

Archive of SID

www.SID.ir

and

$$V=\left[(3w_m-1)\rho_0\, e^{-3A(1+w_m+\delta)(\ln T_1)^{\alpha}}+\frac{3}{4\pi G}\left\{\frac{A\alpha}{T_1^2}(\ln T_1)^{\alpha-2}(\alpha-1+(3\xi-4)\ln T_1+2A\alpha(\ln T_1)^{\alpha})+k\, e^{-2A(\ln T_1)^{\alpha}}\right\}\right]^2$$
$$\times\left[2(w_m-1)\rho_0\, e^{-3A(1+w_m+\delta)(\ln T_1)^{\alpha}}+\frac{1}{2\pi G}\left\{\frac{A\alpha}{T_1^2}(\ln T_1)^{\alpha-2}(\alpha-1+(5\xi-6)\ln T_1+3A\alpha(\ln T_1)^{\alpha})+2k\, e^{-2A(\ln T_1)^{\alpha}}\right\}\right]^{-1}. \quad (50)$$

- For intermediate scenario, we get the expressions for ϕ and V as

$$\phi=\int\left[2(w_m-1)\rho_0\, e^{-3B(1+w_m+\delta)T_1^{\beta}}+\frac{1}{2\pi G}\left\{B\beta(5\xi+\beta-6+3B\beta T_1^{\beta})T_1^{\beta-2}+2k\, e^{-2BT_1^{\beta}}\right\}\right]^{\frac{1}{2}}$$
$$\times\left[(3w_m-1)\rho_0\, e^{-3B(1+w_m+\delta)T_1^{\beta}}+\frac{3}{4\pi G}\left\{B\beta(3\xi+\beta-4+2B\beta T_1^{\beta})T_1^{\beta-2}+k\, e^{-2BT_1^{\beta}}\right\}\right]^{-\frac{1}{2}} dT_1, \quad (51)$$

and

$$V=\left[(3w_m-1)\rho_0\, e^{-3B(1+w_m+\delta)T_1^{\beta}}+\frac{3}{4\pi G}\left\{B\beta(3\xi+\beta-4+2B\beta T_1^{\beta})T_1^{\beta-2}+k\, e^{-2BT_1^{\beta}}\right\}\right]^2$$
$$\times\left[2(w_m-1)\rho_0\, e^{-3B(1+w_m+\delta)T_1^{\beta}}+\frac{1}{2\pi G}\left\{B\beta(5\xi+\beta-6+3B\beta T_1^{\beta})T_1^{\beta-2}+2k\, e^{-2BT_1^{\beta}}\right\}\right]^{-1}. \quad (52)$$

From Figures 7, 8, and 9, we see that for interacting k-essence, the potential V always decreases with the increase in the scalar field ϕ in all of the three scenarios. It happens for open, closed, and flat universes.

Figure 7 Variations of V against k-essence field ϕ in the emergent scenario. Red, green, and blue lines represent $k=-1$, $k=+1$, and $k=0$, respectively.

Figure 8 Variations of V against k-essence field ϕ in the logamediate scenario. Red, green, and blue lines represent $k=-1$, $k=+1$, and $k=0$, respectively.

Figure 9 Variations of V against k-essence field ϕ in the intermediate scenario. Red, green, and blue lines represent $k=-1$, $k=+1$, and $k=0$, respectively.

Dirac-Born-Infeld-essence

Consider that the dark energy scalar field is a DBI scalar field. In this case, the action of the field be written as [58-61]

$$S_{\rm D}=-\int d^4x a^3(t)\left[T(\phi)\sqrt{1-\frac{\dot{\phi}^2}{T(\phi)}}+V(\phi)-T(\phi)\right], \quad (53)$$

where $T(\phi)$ is the warped brane tension, and $V(\phi)$ is the DBI potential. The energy density and pressure of the DBI-essence scalar field are, respectively, given by

$$\rho_{\rm D}=(\gamma-1)T(\phi)+V(\phi) \quad (54)$$

and

$$p_{\rm D}=\frac{\gamma-1}{\gamma}T(\phi)-V(\phi), \quad (55)$$

Archive of SID

www.SID.ir

where γ is given by

$$\gamma = \frac{1}{\sqrt{1-\frac{\dot{\phi}^2}{T(\phi)}}}. \tag{56}$$

Now, we consider here a particular case $\gamma =$ constant. In this case, for simplicity, we assume $T(\phi) = T_0\dot{\phi}^2$ ($T_0 > 1$). So, we have $\gamma = \sqrt{\frac{T_0}{T_0-1}}$. In this case, the expressions for ϕ, $T(\phi)$, and $V(\phi)$ are given by

$$\dot{\phi}^2 = \sqrt{\frac{T_0-1}{T_0}}\left[-(1+w_m)\rho_m + \frac{1}{4\pi G}\left(-\dot{H} + \frac{\xi-1}{T_1}H + \frac{k}{a^2}\right)\right] \tag{57}$$

$$T = \sqrt{T_0(T_0-1)}\left[-(1+w_m)\rho_m + \frac{1}{4\pi G}\left(-\dot{H} + \frac{\xi-1}{t}H + \frac{k}{a^2}\right)\right], \tag{58}$$

and

$$V = \left[\left(T_0 - \sqrt{T_0(T_0-1)}\right)(1+w_m) - w_m\right]\rho_m - \frac{1}{8\pi G}\left[\left(1 - T_0 + \sqrt{T_0(T_0-1)}\right)\dot{H} + 3H^2 \right.$$
$$\left. +2\left(T_0 - \sqrt{T_0(T_0-1)} + 2\right)\frac{\xi-1}{T_1}H + \left(2T_0 - 2\sqrt{T_0(T_0-1)} + 1\right)\frac{k}{a^2}\right]. \tag{59}$$

- For emergent scenario, we get the expressions for ϕ, T, and V as

$$\phi = \left(\frac{T_0-1}{T_0}\right)^{\frac{1}{4}}\int\left[-\frac{(1+w_m)\rho_0 a_0^{-3(1+w_m+\delta)}}{(\lambda+e^{\mu T_1})^{3n(1+w_m+\delta)}} + \frac{1}{4\pi G}\left\{-\frac{n\lambda\mu^2 e^{\mu T_1}}{(\lambda+e^{\mu T_1})^2} + \frac{(\xi-1)n\mu e^{\mu T_1}}{T_1(\lambda+e^{\mu T_1})} + \frac{k\, a_0^{-2}}{(\lambda+e^{\mu T_1})^{2n}}\right\}\right]^{\frac{1}{2}} dT_1, \tag{60}$$

$$T = \sqrt{T_0(T_0-1)}\left[-\frac{(1+w_m)\rho_0 a_0^{-3(1+w_m+\delta)}}{(\lambda+e^{\mu T_1})^{3n(1+w_m+\delta)}} + \frac{1}{4\pi G}\left\{-\frac{n\lambda\mu^2 e^{\mu T_1}}{(\lambda+e^{\mu T_1})^2} + \frac{(\xi-1)n\mu e^{\mu t}}{T_1(\lambda+e^{\mu T_1})} + \frac{k\, a_0^{-2}}{(\lambda+e^{\mu T_1})^{2n}}\right\}\right], \tag{61}$$

and

$$V = \left[\left(T_0 - \sqrt{T_0(T_0-1)}\right)(1+w_m) - w_m\right]\frac{\rho_0 a_0^{-3(1+w_m+\delta)}}{(\lambda+e^{\mu T_1})^{3n(1+w_m+\delta)}} - \frac{1}{8\pi G}\left[\left(1 - T_0 + \sqrt{T_0(T_0-1)}\right)\frac{n\lambda\mu^2 e^{\mu T_1}}{(\lambda+e^{\mu T_1})^2}\right.$$
$$\left. +\frac{3n^2\mu^2 e^{2\mu T_1}}{(\lambda+e^{\mu T_1})^2} + 2\left(T_0 - \sqrt{T_0(T_0-1)} + 2\right)\frac{(\xi-1)}{T_1}\frac{n\mu e^{\mu T_1}}{(\lambda+e^{\mu T_1})} + \left(2T_0 - 2\sqrt{T_0(T_0-1)} + 1\right)\frac{k\, a_0^{-2}}{(\lambda+e^{\mu T_1})^{2n}}\right]. \tag{62}$$

- For logamediate scenario, we get the expressions for ϕ, T, and V as

$$\phi = \left(\frac{T_0-1}{T_0}\right)^{\frac{1}{4}}\int\left[-(1+w_m)\rho_0\, e^{-3A(1+w_m+\delta)(\ln T_1)^\alpha} + \frac{1}{4\pi G}\left\{\frac{A\alpha}{T_1^2}(\ln T_1)^{\alpha-2}(1-\alpha+\xi\ln T_1) + k\, e^{-2A(\ln T_1)^\alpha}\right\}\right]^{\frac{1}{2}} dT_1, \tag{63}$$

$$T = \sqrt{T_0(T_0-1)}\left[-(1+w_m)\rho_0\, e^{-3A(1+w_m+\delta)(\ln T_1)^\alpha} + \frac{1}{4\pi G}\left\{\frac{A\alpha}{T_1^2}(\ln T_1)^{\alpha-2}(1-\alpha+\xi\ln T_1) + k\, e^{-2A(\ln T_1)^\alpha}\right\}\right], \tag{64}$$

and

$$V = \left[\left(T_0 - \sqrt{T_0(T_0-1)}\right)(1+w_m) - w_m\right]\rho_0\, e^{-3A(1+w_m+\delta)(\ln T_1)^\alpha} - \frac{1}{8\pi G}\left[2\left(T_0 - \sqrt{T_0(T_0-1)} + 2\right)\frac{(\xi-1)A\alpha}{T_1^2}(\ln T_1)^{\alpha-1}\right.$$

Archive of SID

www.SID.ir

$$+\frac{3A^2\alpha^2}{T_1^2}(\ln T_1)^{2\alpha-2}+\left(1-T_0+\sqrt{T_0(T_0-1)}\right)\frac{A\alpha}{T_1^2}(\ln T_1)^{\alpha-2}(\alpha-1-\ln T_1)+\left(2T_0-2\sqrt{T_0(T_0-1)}+1\right)k\,e^{-2A(\ln T_1)^{\alpha}}\Bigg]. \tag{65}$$

- For intermediate scenario, we get the expressions for ϕ, T, and V as

$$\phi=\left(\frac{T_0-1}{T_0}\right)^{\frac{1}{4}}\int\left[-(1+w_m)\rho_0\,e^{-3B(1+w_m+\delta)T_1^{\beta}}+\frac{1}{4\pi G}\left\{B\beta(\xi-\beta)T_1^{\beta-2}+k\,e^{-2BT_1^{\beta}}\right\}\right]^{\frac{1}{2}}dT_1, \tag{66}$$

$$T=\sqrt{T_0(T_0-1)}\left[-(1+w_m)\rho_0\,e^{-3B(1+w_m+\delta)T_1^{\beta}}+\frac{1}{4\pi G}\left\{B\beta(\xi-\beta)T_1^{\beta-2}+k\,e^{-2BT_1^{\beta}}\right\}\right], \tag{67}$$

and

$$V=\left[\left(T_0-\sqrt{T_0(T_0-1)}\right)(1+w_m)-w_m\right]\rho_0\,e^{-3B(1+w_m+\delta)T_1^{\beta}}-\frac{1}{8\pi G}\left[\left(1-T_0+\sqrt{T_0(T_0-1)}\right)B\beta(\beta-1)T_1^{\beta-2}\right.$$
$$\left.+3B^2\beta^2T_1^{2\beta-2}+2\left(T_0-\sqrt{T_0(T_0-1)}+2\right)\frac{(\xi-1)}{T_1}B\beta T_1^{\beta-1}+\left(2T_0-2\sqrt{T_0(T_0-1)}+1\right)k\,e^{-2BT_1^{\beta}}\right]. \tag{68}$$

When we consider an interacting DBI-essence dark energy, we get a decaying pattern in the V-ϕ plot for emergent and intermediate scenarios in the Figures 10 and 11, respectively. However, from Figure 12, we see an increasing plot of V-ϕ for interacting DBI-essence in the logamediate scenario.

Figure 10 Variations of V against DBI field ϕ in the emergent scenario. Solid, dash, and dotted lines represent $k=-1$, $k=+1$, and $k=0$, respectively.

Figure 11 Variations of V against DBI field ϕ in the intermediate scenario. Solid, dash, and dotted lines represent $k=-1$, $k=+1$, and $k=0$, respectively.

Figure 12 Variations of V against DBI field ϕ in the logamediate scenario. Solid, dash, and dotted lines represent $k=-1$, $k=+1$, and $k=0$, respectively.

Hessence

Wei et al. [62,63] proposed a novel non-canonical complex scalar field named 'hessence' which plays the role of quintom. In the hessence model, the so called internal motion $\dot{\theta}$, where θ is the internal degree of freedom of hessence, which plays a phantom-like role. The phantom divide transitions are also possible. The Lagrangian density of the hessence is given by

$$\mathcal{L}_{\rm h}=\frac{1}{2}[(\partial_\mu\phi)^2-\phi^2(\partial_\mu\theta)^2]-V(\phi). \tag{69}$$

The pressure and energy density for the hessence model are given by

$$p_{\rm h}=\frac{1}{2}(\dot{\phi}^2-\phi^2\dot{\theta}^2)-V(\phi), \tag{70}$$

and

$$\rho_{\rm h}=\frac{1}{2}(\dot{\phi}^2-\phi^2\dot{\theta}^2)+V(\phi), \tag{71}$$

with

$$Q=a^3\phi^2\dot{\theta}=\text{constant}, \tag{72}$$

Archive of SID

www.SID.ir

where Q is the total conserved charge, ϕ is the hessence scalar field, and V is the corresponding potential. Equation (71) is conserved, but in FAC (proposed in [4,5]), there is a violation of energy, charge, and the Noether symmetry theorem. For reference, see [64-66].

From above, we get

$$\dot{\phi}^2 - \frac{Q^2}{a^6\phi^2} = -(1+w_m)\rho_m + \frac{1}{4\pi G}\left(-\dot{H} + \frac{\xi-1}{T_1}H + \frac{k}{a^2}\right), \tag{73}$$

and

$$V = \frac{1}{2}(w_m-1)\rho_m + \frac{1}{8\pi G}\left(\dot{H} + 3H^2 + \frac{5(\xi-1)}{T_1}H + \frac{2k}{a^2}\right). \tag{74}$$

- For emergent scenario, we get the expressions for ϕ and V as

$$\dot{\phi}^2 - \frac{Q^2}{a_0^6\left(\lambda+e^{\mu T_1}\right)^{6n}\phi^2} = -\frac{(1+w_m)\rho_0 a_0^{-3(1+w_m+\delta)}}{\left(\lambda+e^{\mu T_1}\right)^{3n(1+w_m+\delta)}} + \frac{1}{4\pi G}\left\{-\frac{n\lambda\mu^2 e^{\mu T_1}}{\left(\lambda+e^{\mu T_1}\right)^2} + \frac{(\xi-1)n\mu e^{\mu t}}{T_1(\lambda+e^{\mu T_1})} + \frac{k\,a_0^{-2}}{\left(\lambda+e^{\mu T_1}\right)^{2n}}\right\}, \tag{75}$$

and

$$V = \frac{(w_m-1)\rho_0 a_0^{-3(1+w_m+\delta)}}{2\left(\lambda+e^{\mu T_1}\right)^{3n(1+w_m+\delta)}} + \frac{1}{8\pi G}\left\{\frac{n\mu^2 e^{\mu T_1}(\lambda+3ne^{\mu T_1})}{\left(\lambda+e^{\mu T_1}\right)^2} + \frac{5(\xi-1)n\mu e^{\mu T_1}}{T_1(\lambda+e^{\mu T_1})} + \frac{2k\,a_0^{-2}}{\left(\lambda+e^{\mu T_1}\right)^{2n}}\right\}. \tag{76}$$

- For logamediate scenario, we get the expressions for ϕ and V as

$$\dot{\phi}^2 - \frac{Q^2 e^{-6A(\ln T_1)^\alpha}}{\phi^2} = -(1+w_m)\rho_0\, e^{-3A(1+w_m+\delta)(\ln T_1)^\alpha} + \frac{1}{4\pi G}\left\{\frac{A\alpha}{T_1^2}(\ln T_1)^{\alpha-2}(1-\alpha+\xi\ln T_1) + k\, e^{-2A(\ln T_1)^\alpha}\right\} \tag{77}$$

and

$$V = \frac{(w_m-1)\rho_0}{2}\, e^{-3A(1+w_m+\delta)(\ln T_1)^\alpha} + \frac{1}{8\pi G}\left[\frac{A\alpha}{T_1^2}(\ln T_1)^{\alpha-2}\{\alpha-1+(5\xi-6)\ln T_1 + 3A\alpha(\ln T_1)^\alpha\} + 2k\, e^{-2A(\ln T_1)^\alpha}\right]. \tag{78}$$

- For intermediate scenario, we get the expressions for ϕ and V as

$$\dot{\phi}^2 - \frac{Q^2 e^{-6BT_1^\beta}}{\phi^2} = -(1+w_m)\rho_0\, e^{-3B(1+w_m+\delta)T_1^\beta} + \frac{1}{4\pi G}\left\{B\beta(\xi-\beta)T_1^{\beta-2} + k\, e^{-2BT_1^\beta}\right\}, \tag{79}$$

and

$$V = \frac{(w_m-1)\rho_0}{2}\, e^{-3B(1+w_m+\delta)T_1^\beta} + \frac{1}{8\pi G}\left[B\beta T_1^{\beta-2}(5\xi+\beta+3B\beta T_1^\beta) + 2k\, e^{-2BT_1^\beta}\right]. \tag{80}$$

For interacting hessence dark energy, Figure 13 shows an increase in the potential with scalar field. Figures 14 and 15 show decay in the potential with scalar field. This means that the potential for interacting hessence increases in the emergent universe and decays in logamediate and intermediate scenarios.

Archive of SID

www.SID.ir

Figure 13 Variations of V against hessence field ϕ in the emergent scenario. Red, green, and blue lines represent $k = -1$, $k = +1$, and $k = 0$, respectively.

Figure 14 Variations of V against hessence field ϕ in the logamediate scenario. Red, green, and blue lines represent $k = -1$, $k = +1$, and $k = 0$, respectively.

Figure 15 Variations of V against hessence field ϕ in the intermediate scenario. Red, green, and blue lines represent $k = -1$, $k = +1$, and $k = 0$, respectively.

Dilaton field

Phantom field with a negative kinetic term has a problem with quantum instabilities [29]. Copeland et al. [29] reviewed the issues that led to the introduction of dilaton dark energy. The energy density and pressure of the dilaton dark energy model are given by [29]

$$\rho_{\rm d} = -X + 3Ce^{\lambda\phi}X^2 \tag{81}$$

and

$$p_{\rm d} = -X + Ce^{\lambda\phi}X^2, \tag{82}$$

respectively, where ϕ is the dilaton scalar field having a kinetic energy $X = \frac{1}{2}\dot{\phi}^2$, λ is the characteristic length which governs all non-gravitational interactions of the dilaton, and C is a positive constant.

We get

$$\phi = \int \left[\frac{1}{2}(3w_m - 1)\rho_m + \frac{3}{8\pi G}\left(\dot{H} + 2H^2 + \frac{3(\xi-1)}{T_1}H + \frac{k}{a^2}\right)\right]^{\frac{1}{2}} dT_1. \tag{83}$$

- For emergent scenario, we have

$$\phi = \int \left[\frac{(3w_m - 1)\rho_0 a_0^{-3(1+w_m+\delta)}}{2\left(\lambda + e^{\mu T_1}\right)^{3n(1+w_m+\delta)}} + \frac{3}{8\pi G}\left\{\frac{n\mu^2 e^{\mu T_1}(\lambda + 2ne^{\mu T_1})}{\left(\lambda + e^{\mu T_1}\right)^2} + \frac{3(\xi-1)n\mu e^{\mu T_1}}{T_1(\lambda + e^{\mu T_1})} + \frac{k\, a_0^{-2}}{\left(\lambda + e^{\mu T_1}\right)^{2n}}\right\}\right]^{\frac{1}{2}} dT_1. \tag{84}$$

- For logamediate scenario, we get

$$\phi = \int \left[\frac{3}{8\pi G}\left\{\frac{A\alpha}{T_1^2}(\ln T_1)^{\alpha-2}(\alpha - 1 + (3\xi - 4)\ln T_1 + 2A\alpha(\ln T_1)^{\alpha}) + k\, e^{-2A(\ln T_1)^{\alpha}}\right\} + \frac{1}{2}(3w_m - 1)\rho_0\, e^{-3A(1+w_m+\delta)(\ln T_1)^{\alpha}}\right]^{\frac{1}{2}} dT_1. \tag{85}$$

- For intermediate scenario, we get

$$\phi = \int \left[\frac{1}{2}(3w_m - 1)\rho_0\, e^{-3B(1+w_m+\delta)T_1^{\beta}} + \frac{3}{8\pi G}\left\{B\beta(3\xi + \beta - 4 + 2B\beta T_1^{\beta})T_1^{\beta-2} + k\, e^{-2BT_1^{\beta}}\right\}\right]^{\frac{1}{2}} dT_1. \tag{86}$$

For interacting dilaton field, the scalar field ϕ always increases with cosmic time T_1, irrespective of the scenario of the universe we consider. This is displayed in Figures 16, 17, and 18 for emergent, logamediate, and intermediate scenarios, respectively.

Archive of SID

www.SID.ir

Figure 16 Variations of dilaton field ϕ against time T_1 in the emergent scenario. Red, green, and blue lines represent $k = -1$, $k = +1$, and $k = 0$, respectively.

Figure 17 Variations of dilaton field ϕ against time T_1 in the logamediate scenario. Red, green, and blue lines represent $k = -1$, $k = +1$, and $k = 0$, respectively.

Figure 18 Variations of dilaton field ϕ against time T_1 in the intermediate scenario. Red, green, and blue lines represent $k = -1$, $k = +1$, and $k = 0$, respectively.

Yang-Mills dark energy

Recent studies suggest that Yang-Mills field can be considered as a useful candidate to describe the dark energy. As in the normal scalar models, the connection of field to particle physics models has not been clear so far, and the weak energy condition cannot be violated by the field. In the effective Yang-Mills condensate (YMC) dark energy model, the effective Yang-Mills field Lagrangian is given by [67-69]

$$\mathcal{L}_{\rm YMC} = \frac{1}{2} bF(\ln\left|\frac{F}{K^2}\right| - 1), \tag{87}$$

where K is the re-normalization scale of dimension of squared mass. F plays the role of the order parameter of the YMC where, F is given by $F = -\frac{1}{2}F^a_{\mu\nu}F^{a\mu\nu} = E^2 - B^2$. The pure electric case we have is $B = 0$, i.e., $F = E^2$.

From the above Lagrangian, we can derive the energy density and the pressure of the YMC in the flat FRW spacetime as

$$\rho_{\rm y} = \frac{1}{2}(y+1)bE^2 \tag{88}$$

and

$$p_{\rm y} = \frac{1}{6}(y-3)bE^2, \tag{89}$$

respectively, where y is defined as,

$$y = \ln\left|\frac{E^2}{K^2}\right|. \tag{90}$$

We get

$$E^2 = \left[\frac{1}{2b}(3w_m - 1)\rho_m + \frac{3}{8\pi Gb}\left(\dot{H} + 2H^2 + \frac{3(\xi-1)}{T_1}H + \frac{k}{a^2}\right)\right]. \tag{91}$$

- For emergent scenario, we have

$$E^2 = \left[\frac{(3w_m-1)\rho_0 a_0^{-3(1+w_m+\delta)}}{2b\left(\lambda + e^{\mu T_1}\right)^{3n(1+w_m+\delta)}} + \frac{3}{8\pi bG}\left\{\frac{n\mu^2 e^{\mu T_1}(\lambda + 2ne^{\mu T_1})}{\left(\lambda + e^{\mu T_1}\right)^2} + \frac{3(\xi-1)n\mu e^{\mu T_1}}{T_1(\lambda + e^{\mu T_1})} + \frac{k\, a_0^{-2}}{(\lambda + e^{\mu T_1})^{2n}}\right\}\right]. \tag{92}$$

- For logamediate scenario, we get

$$E^2 = \left[\frac{3}{8\pi bG}\left\{\frac{A\alpha}{T_1^2}(\ln T_1)^{\alpha-2}(\alpha - 1 + (3\xi - 4)\ln T_1 + 2A\alpha(\ln T_1)^\alpha) + k\, e^{-2A(\ln T_1)^\alpha}\right\}\right.$$
$$\left. + \frac{1}{2b}(3w_m - 1)\rho_0\, e^{-3A(1+w_m+\delta)(\ln T_1)^\alpha}\right]. \tag{93}$$

Archive of SID

www.SID.ir

- For intermediate scenario, we get

$$E^2 = \left[\frac{1}{2b}(3w_m - 1)\rho_0\, e^{-3B(1+w_m+\delta)T_1^{\beta}} + \frac{3}{8\pi bG}\left\{B\beta(3\xi + \beta - 4 + 2B\beta T_1^{\beta})T_1^{\beta-2} + k\, e^{-2BT_1^{\beta}}\right\}\right]. \tag{94}$$

When we consider Yang-Mills dark energy, we find that E^2 is always increasing with cosmic time T_1. This is displayed in Figures 19, 20, and 21 for emergent, logamediate, and intermediate scenarios, respectively.

Figure 19 Variations of E^2 against time T_1 in the emergent scenario. Red, green, and blue lines represent $k = -1$, $k = +1$, and $k = 0$, respectively.

Figure 20 Variations of E^2 against time T_1 in the logamediate scenario. Red, green, and blue lines represent $k = -1$, $k = +1$, and $k = 0$, respectively.

Figure 21 Variations of E^2 against time T_1 in the intermediate scenario. Red, green, and blue lines represent $k = -1$, $k = +1$, and $k = 0$, respectively.

Conclusion

This paper is dedicated to the study of the reconstruction of scalar fields and their potentials in a newly developed model of fractional action cosmology by El-Nabulsi [4,5]. The FAC was constructed by means of Riemann-Liouville fractional integral. Also, it is possible to construct FAC by means of Erdeyi-Kober fractional integral for example or hyperdifferential non-local operators. Detailed discussion on these are available in [70-73]. The fields that we used are quintessence, phantom, tachyonic, k-essence, DBI-essence, hessence, dilaton field, and Yang-Mills field. We assumed that these fields interact with the matter. These fields are various options to model dark energy which is varying in density and pressure, the so called variable dark energy. Different field models possess various advantages and disadvantages. The reconstruction of the field potential involves solving the Friedmann equations in the FAC model with the standard energy densities and pressures of the fields, thereby solving for the field and the potential. For simplicity, we expressed these complicated expressions explicitly in time-dependent form. We plotted these expressions in various figures throughout the paper.

In plotting the figures for various scenarios, we choose the following values: For the emergent scenario, the values are $\xi = 0.6$, $n = 4$, $\lambda = 8$,$\mu = 0.4$, $a_0 = 0.7$, and $G = 1$ (all DE models); for logamediate $\xi = 0.6$, $\alpha = 3$, $A = 5$, and $G = 1$ (all DE models); and for intermediate $\xi = 0.6$, $\beta = 0.4$, $B = 2$, and $G = 1$ (all DE models). 0 Moreover, in all cases $\delta = 0.05$, $w_m = 0.01$. In Figures 1, 2, and 3, we show the variations of V against ϕ in the emergent, logamediate, and intermediate scenarios, respectively for phantom and quintessence field. In the first two cases, the potential function is a decreasing function of the field. For the quintessence field, the potential is almost constant, while for the phantom field, the potential increases for different field values. Figures 4, 5, and 6 show the variations of V against ϕ in the emergent, logamediate, and intermediate scenarios, respectively for the tachyonic field. In Figure 4, the V-ϕ plot for normal tachyon and phantom tachyon models of dark energy is presented for emergent scenario of the universe. Potential of normal tachyon exhibits decaying pattern. However, it shows an increasing pattern for phantom tachyonic field ϕ. It happens irrespective of the curvature of the universe. In the logamediate scenario (Figure 5), the potentials for normal tachyon and phantom tachyon exhibit increasing and decreasing behaviors, respectively, with increase in the scalar field ϕ. From Figure 6, we see a continuous decay in the potential for normal tachyonic field in the intermediate scenario. However, in this scenario, the behavior of the potential varies with the curvature of the universe characterized by

Archive of SID

www.SID.ir

interacting phantom tachyonic field. For $k = -1$ and $k = 1$, the potential increases with phantom tachyonic field, and for $k = 0$, it decays after increasing initially.

Similarly, Figures 7, 8, and 9 show the reconstructed potentials for the k-essence field. We have seen that for interacting k-essence, the potential V always decreases with the increase in the scalar field ϕ in all of the three scenarios, and it happens for open, closed, and flat universes. When we consider an interacting DBI-essence dark energy, we get a decaying pattern in the V-ϕ plot for emergent and intermediate scenarios in the Figures 10 and 11. However, from Figure 12, we see an increasing plot of V-ϕ for interacting DBI-essence in the logamediate scenario. For interacting hessence dark energy, Figure 13 shows an increase in the potential with scalar field, and Figures 14 and 15 show decay in the potential with scalar field. This means that the potential for interacting hessence increases in the emergent universe and decays in logamediate and intermediate scenarios. Figures 16, 17, and 18 discuss the dilaton field, while Figures 19, 20, and 21 show the behavior of the Yang-Mills field in the FAC. For interacting dilaton field, the scalar field ϕ always increases with cosmic time T_1, irrespective of the scenario of the universe. When we consider Yang-Mills dark energy, we find that E^2 is always increasing with cosmic time T_1.

Since the emergent, logamediate, and intermediate expansions derive accelerating model of the universe, different types of dark energy models give the nature of their scalar field and potential in different phases of the expansion. For the emergent scenario, the potentials are increasing for hessence and tachyonic fields, but are decreasing for quintessence, phantom, k-essence, and DBI-essence models. For the logamediate scenario, the potentials are increasing for tachyon and DBI-essence models. However, in this scenario, the potentials are decreasing for quintessence, phantom, and k-essence models. For the intermediate scenario, the potentials are increasing for phantom and tachyonic field, but are decaying for k-essence, hessence, and DBI-essence models. Thus, the increasing or decreasing nature of the potentials of all dark energy models completely depend on the expansion nature of the universe.

Competing interests

The authors declare that they have no competing interests.

Authors' contributions

UD conceived the idea of the work. Computations have been carried out jointly by UD, SC, and MJ. The plotting was made by SC. The text has been written jointly by UD, SC, and MJ. All authors read and approved the final manuscript.

Authors' information

The first author UD obtained his BSc in Mathematics (with honors) from Jadavpur University (JU), India in 1997 and MSc in Mathematics from the same university in 1999. Subsequently, he qualified in the National Eligibility Test conducted jointly by the University Grants Commission of India and the Council of Scientific and Industrial Research of India, and carried out his research work in the Department of Mathematics of JU and received his PhD (Science) degree in Mathematics in 2004. Presently, UD is working as an Assistant Professor in the Department of Mathematics of the Bengal Engineering Science University, Shibpur, India. Also, UD is a Visiting Associate of the Inter-University Centre for Astronomy and Astrophysics (IUCAA), Pune, India and Third World Academy of Science (TWAS), Trieste, Italy. He is actively engaged in research in the area of Relativity and Cosmology. UD has more than 100 papers to his credit published in various peer-reviewed journals of repute. UD has acted as a reviewer in different journals related to the areas of Relativity and Cosmology.

Archive of SID

www.SID.ir

The second author SC completed his MSc in Mathematics from Jadavpur University, Calcutta (India) in 1999 and PhD (Science) in Mathematics from Bengal Engineering and Science University, Shibpur (India) in 2010. He is a Visiting Associate of the Inter-University Centre for Astronomy and Astrophysics (IUCAA), Pune (India) since August 2011. He is working as an Assistant Professor of Mathematics at Pailan College of Management and Technology, Kolkata, India since 2006. His areas of research interest include dark energy models and modified gravity theories. The author is having 72 research papers published in various peer-reviewed journals.

The third author MJ obtained MSc degree in Mathematics from Quaid-e-Azam University, Islamabad (Pakistan) in 2004 and PhD in Mathematics from National University of Science and Technology, Islamabad (Pakistan) in 2010. Presently, he is working as an Assistant Professor at the Center for Advanced Mathematics and Physics, National University of Sciences and Technology, Islamabad, Pakistan. He is a Visiting Associate of the Third World Academy of Science (TWAS), Trieste, Italy. His areas of research interest include dark energy models, thermodynamics, and modified gravity theories. The author is having more than 70 research papers published in various peer-reviewed journals. Also, MJ has acted as a reviewer in different journals in the areas of Cosmology and Astrophysics.

Acknowledgments

We are expressing our gratitude to the anonymous reviewers for giving constructive suggestions to enhance the quality of the manuscript. The first two authors (UD and SC) sincerely acknowledge the Inter-University Centre for Astronomy and Astrophysics (IUCAA), Pune for providing Visiting Associateship to carry out research in Cosmology. The second author (SC) duly acknowledges the financial support from the DST, Government of India under the project grant no. SR/FTP/PS-167/2011.

References

1. Podlubny, I: An Introduction to Fractional Derivatives, Fractional Differential Equations, to Methods of Their Solution and Some of Their Applications. Academic Press, New York (1999)

2. Robert, M: Fractional derivative cosmology. arXiv:0909.1171 [gr-qc]. http://arxiv.org/abs/0909.1171 (2013). Accessed 20 May 2013

3. Shchigolev, VK: Cosmological models with fractional derivatives and fractional action functional. Commun. Theor. Phys. **56**, 389–396 (2011)

4. El-Nabulsi, RA: Gravitons in fractional action cosmology. Int. J. Theor. Phys. **51**, 3978–3992 (2012)

5. El-Nabulsi, RA: Cosmology with a fractional action principle. Rom. Rep. Phys. **59**(3), 763–771 (2007)

6. EL-Nabulsi, RA: Oscillating flat FRW dark energy dominated cosmology from periodic functional approach. Commun. Theor. Phys. **54**, 16 (2010)

7. Jamil, M, Momeni, D, Rashid, MA: Fractional action cosmology with power law weight function. J. Phys. Conf. Ser. **354**, 012008 (2012)

8. Farooq, MU, Jamil, M, Debnath, U: Dynamics of interacting phantom and quintessence dark energies. Astrophys. Space Sci. **334**, 243 (2011)

9. Debnath, U, Jamil, M: Correspondence between DBI-essence and modified Chaplygin gas and the generalized Second Law of Thermodynamics. Astrophys. Space Sci. **335**, 545 (2011)

Archive of SID

www.SID.ir

10. Karami, K, Khaledian, MS, Jamil, M: Reconstructing interacting entropy-corrected holographic scalar field models of dark energy in the non-flat universe. Phys. Scr. **83**, 025901 (2011)

11. Setare, MR, Jamil, M: Correspondence between entropy-corrected holographic and Gauss-Bonnet dark energy models. Europhys. Lett. **92**, 49003 (2010)

12. Sheykhi, A, Jamil, M: Interacting HDE and NADE in Brans-Dicke chameleon cosmology. Phys. Lett. B. **694**, 284 (2011)

13. Jamil, M, Karami, K, Sheykhi, A: Restoring new agegraphic dark energy in RS II braneworld. Int. J. Theor. Phys. **50**, 3069 (2011)

14. Farooq, MU, Jamil, M, Rashid, MA: Interacting entropy-corrected new agegraphic K-essence, tachyon and dilaton scalar field models in non-flat universe. Int. J. Theor. Phys. **49**, 2278 (2010)

15. Jamil, M, Sheykhi, A, Farooq, MU: Thermodynamics of interacting entropy-corrected holographic dark energy in a non-flat FRW universe. Int. J. Mod. Phys. D. **19**, 1831 (2010)

16. Setare, MR, Saridakis, EN: Correspondence between holographic and GaussŰBonnet dark energy models. Phys. Lett. B. **670**, 1 (2008)

17. Barrow, JD, Nunes, NJ: Dynamics of "logamediate" inflation. Phys. Rev. D. **76**, 043501 (2007)

18. Campuzano, C, del Campo, S, Herrera, R, Rojas, E, Saavedra, J: Curvaton reheating in a logamediate inflationary model. Phys. Rev. D. **80**, 123531 (2009)

19. Paul, BC, Thakur, P, Ghose, S: Constraints on exotic matter needed for an emergent universe. Mon. Not. Roy. Astron. Soc. **407**, 415 (2010)

20. Ellis, GFR, Murugan, J, Tsagas, CG: The emergent universe: an explicit construction. Class. Quant. Grav. **21**, 233 (2004)

21. Laughlin, RB: Emergent relativity. Int. J. Mod. Phys. A. **18**, 831 (2003)

22. Khatua, PB, Debnath, U: Dynamics of logamediate and intermediate scenarios in the dark energy filled universe. Int. J. Theor. Phys. **50**, 799 (2011)

23. Capozziello, S, Nesseris, S, Perivolaropoulos, L: Reconstruction of the scalar-tensor Lagrangian from a LCDM background and Noether symmetry. JCAP **0712**, 009 (2007)

24. Capozziello, S, Piedipalumbo, E, Rubano, C, Scudellaro, P: Noether symmetry approach in phantom quintessence cosmology. Phys. Rev. D. **80**, 104030 (2009)

25. He, J-H, Wang, B, Zhang, P: Imprint of the interaction between dark sectors in large scale cosmic microwave background anisotropies. Phys. Rev. D. **80**, 063530 (2009)

26. He, J-H, Wang, B, Jing, YP: Effects of dark sectors' mutual interaction on the growth of structures. JCAP **0907**, 030 (2009)

27. Chattopadhyay, S, Debnath, U: Role of generalized Ricci dark energy on Chameleon field in the emergent universe. Can. J. Phys. **89**(9), 941 (2011)

28. Mukherjee, S, Paul, BC, Dadhich, NK, Maharaj, SD, Beesham, A: Emergent universe with exotic matter class. Quantum Grav. **23**, 6927 (2006)

29. Copeland, EJ, Sami, M, Tsujikawa, S: Dynamics of dark energy. Int. J. Mod. Phys. D. **15**, 1753 (2006)

Archive of SID

www.SID.ir

30. Amendola, L: Phantom energy mediates a long-range repulsive force. Phys. Rev. Lett. **93**, 181102 (2004)

31. Bronikov, KA: Scalar-tensor theory and scalar charge. Acta Phys. Polon. B. **4**, 251 (1973)

32. Ellis, HG: Ether flow through a drainhole: a particle model in general relativity. J. Math. Phys. **14**, 104 (1973)

33. Picón, CA: On a class of stable, traversable Lorentzian wormholes in classical general relativity. Phys. Rev. D. **65**, 104010 (2002)

34. Rahaman, F, Kalam, M, Bhui, BC, Chakraborty, S: Construction of a 3D wormhole supported by phantom energy. Phys. Scr. **76**, 56 (2007)

35. Kuhfittig, PK: Seeking exactly solvable models of traversable wormholes supported by phantom energy. Class. Quantum Grav. **23**, 5853 (2006)

36. Babichev, E, Dokuchaev, V, Eroshenko, Y: Black hole mass decreasing due to phantom energy accretion. Phys. Rev. Lett. **93**, 021102 (2004)

37. Nesseris, S, Perivolaropoulos, L: Fate of bound systems in phantom and quintessence cosmologies. Phys. Rev. D. **70**, 123529 (2004)

38. Mota, DF, van de Bruck, C: On the spherical collapse model in dark energy cosmologies. Astron. Astrophs. **421**, 71 (2004)

39. Clifton, T, Mota, DF, Barrow, JD: Inhomogeneous gravity. Mon. Not. Roy. Astron. Soc. **358**, 601 (2005)

40. Babichev, E, Chernov, S, Dokuchaev, V, Eroshenko, Y: Perfect fluid and scalar field in the Reissner-Nordström metric. J. Exp. Theor. Phys. **112**, 784–793 (2011)

41. Babichev, E, Chernov, S, Dokuchaev, V, Eroshenko, Y: Ultrahard fluid and scalar field in the Kerr-Newman metric. Phys. Rev. D. **78**, 104027 (2008)

42. Caldwell, RR, Kamionkowski, M, Weinberg, NN: Phantom energy: dark energy with $w < -1$ causes a cosmic doomsday. Phys. Rev. Lett. **91**, 071301 (2003)

43. Xu, L: Holographic dark energy model with Hubble horizon as an IR cut-off. JCAP **09**, 016 (2009)

44. Gibbons, GW: Cosmological evolution of the rolling tachyon. Phys. Lett. B. **537**, 1 (2002)

45. Mazumdar, A, Panda, S, Perez-Lorenzana, A: Assisted inflation via tachyon condensation. Nucl. Phys. B. **614**, 101 (2001)

46. Feinstein, A: Power-law inflation from the rolling tachyon. Phys. Rev. D. **66**, 063511 (2002)

47. Piao, YS, Cai, RG, Zhang, XM, Zhang, YZ: Assisted tachyonic inflation. Phys. Rev. D. **66**, 121301 (2002)

48. Padmanabhan, T: Accelerated expansion of the universe driven by tachyonic matter. Phys. Rev. D. **66**, 021301 (2002)

49. Bagla, JS, Jassal, HK, Padmanabhan, T: Cosmology with tachyon field as dark energy. Phys. Rev. D. **67**, 063504 (2003)

50. Guo, ZK, Zhang, YZ: Cosmological scaling solutions of multiple tachyon fields with inverse square potentials. JCAP **0408**, 010 (2004)

Archive of SID

www.SID.ir

51. Copeland, EJ, Garousi, MR, Sami, M, Tsujikawa, S: What is needed of a tachyon if it is to be the dark energy? Phys. Rev. D. **71**, 043003 (2005)

52. Armendariz-Picon, C, Damour, T, Mukhanov, VF: k-inflation. Phys. Lett. B. **458**, 209 (1999)

53. Armendariz-Picon, C, Mukhanov, VF, Steinhardt, PJ: Essentials of k-essence. Phys. Rev. D. **63**, 103510 (2001)

54. Armendariz-Picon, C, Mukhanov, VF, Steinhardt, PJ: Dynamical solution to the problem of a small cosmological constant and late-time cosmic acceleration. Phys. Rev. Lett. **85**, 4438 (2000)

55. Chiba T, Okabe T, Yamaguchi M: Kinetically driven quintessence. Phys. Rev. D. **62**, 023511 (2000)

56. Myrzakulov, R: Fermionic K-essence. arXiv:1011.4337. http://arxiv.org/abs/1011.4337 (2013). Accessed 20 May 2013

57. Myrzakulov, R: $F(T)$ gravity and k-essence. Gen. Relat. Gravit. **44**(12), 3059–3080 (2012)

58. Cai, Y-F, Dent, JB, Easson, DA: Warm Dirac-Born-Infeld inflation. Phys. Rev. D. **83**, 101301 (2011)

59. Chattopadhyay, S, Debnath, U: Generalized second law of thermodynamics in presence of interacting DBI essence and other dark energies. Int. J. Mod. Phys. A. **25**, 5557 (2010)

60. Chattopadhyay, S, Debnath, U: Interaction Between DBI-essence and other dark energies. Int. J. Theor. Phys. **49**, 1465 (2010)

61. Ahn, C, Kim, C, Linder, EV: Dark energy properties in DBI theory. Phys. Rev. D. **80**, 123016 (2009)

62. Wei, H, Cai, R-G, Zeng, D-F: Hessence: a new view of quintom dark energy. Class. Quant. Grav. **22**, 3189 (2005)

63. Wei, H, Cai, R-G: Cosmological evolution of "hessence" dark energy and avoidance of the big rip. Phys. Rev. D. **72**, 123507 (2005)

64. El-Nabulsi, RA: A fractional approach to non-conservative Lagrangian dynamical systems. Fiz. A. **14**(4), 289 (2005)

65. El-Nabulsi, RA: A fractional action-like variational approach of some classical, quantum and geometrical dynamics. Int. J. Appl. Math. **17**, 299 (2005)

66. El-Nabulsi, RA: General relativity and quantum field theory: an analysis using fractional functional and action. Int. J. Appl. Math. **18**(2), 235 (2005)

67. Zhang, Y, Xia, TY, Zhao, W: Yang-Mills condensate dark energy coupled with matter and radiation. Class. Quant. Grav. **24**, 3309 (2007)

68. Xia, TY, Zhang, Y: 2-loop quantum Yang-Mills condensate as dark energy. Phys. Lett. B. **656**, 19 (2007)

69. Tong, M, Zhang, Y, Xia, T: Statefinder parameters for quantum effective Yang-Mills condensate dark energy model. Int. J. Mod. Phys. D. **18**, 797 (2009)

70. El-Nabulsi, RA: Fractional derivatives generalizations of Einstein's field equations. Indian J. Phys. **87**(2), 195–200 (2013). doi:10.1007/s12648-012-0201-4

71. El-Nabulsi AR: Calculus of variations with hyperdifferential operators from Tabasaki-Takebe-Toda lattice arguments. Revista de la Real Academia de Ciencias Exactas, Fisicas Y Naturales. Serie A. Mathematicas (2013). doi:10.1007/s13398-012-0086-2

Archive of SID

www.SID.ir

72. El-Nabulsi, RA: The fractional calculus of variations from extended Erdelyi-Kober operator. Int. J. Mod. Phys. B. **23**(16), 3349–3361 (2009)

73. El-Nabulsi, RA: Non-linear dynamics with non-standard Lagrangians. Qual. Theory Dyn. Syst. (2012). doi:10.2007/s12346-012-0074-0

Archive of SID

www.SID.ir

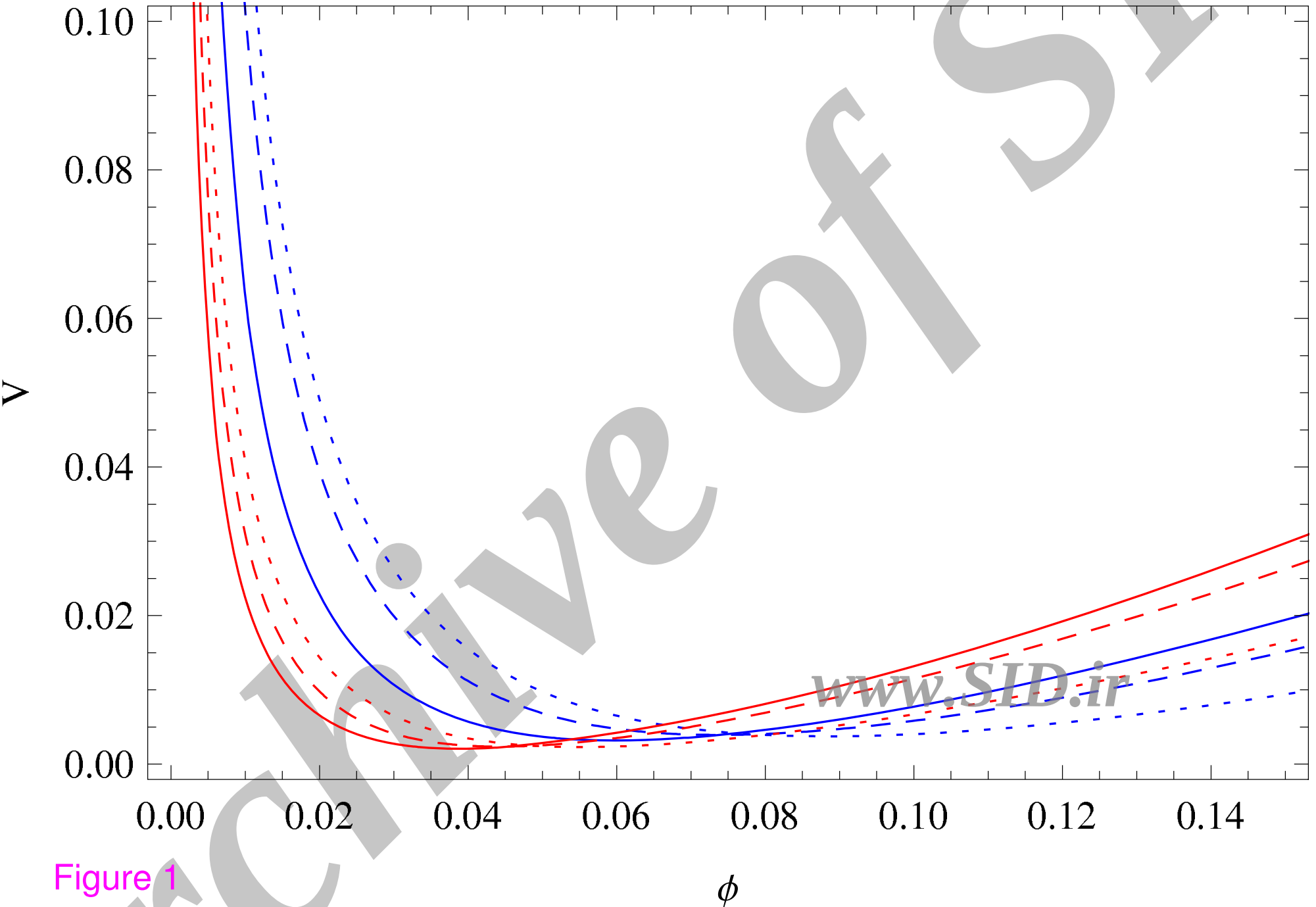

Figure 1

Archive of SID
www.SID.ir

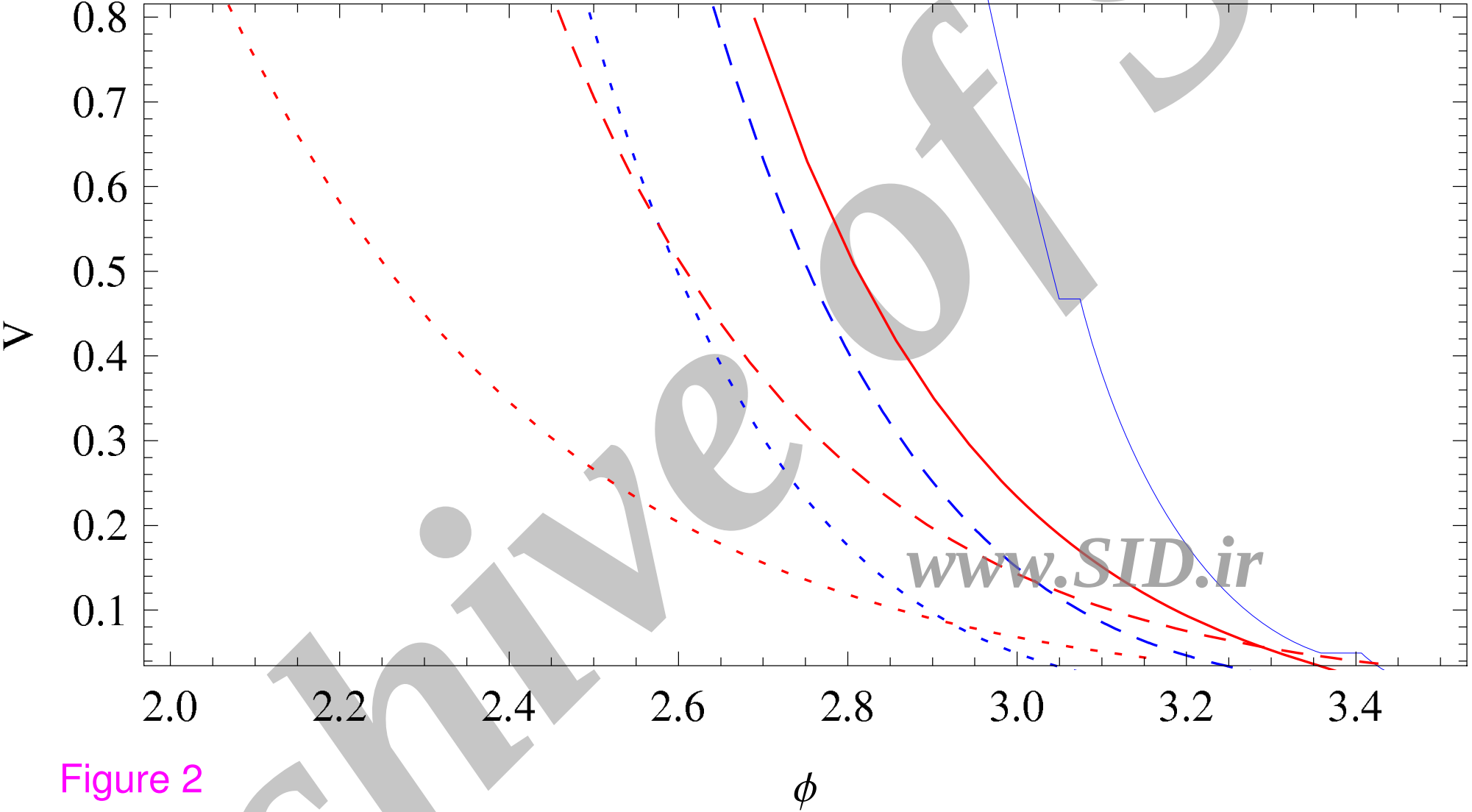

Figure 2

www.SID.ir

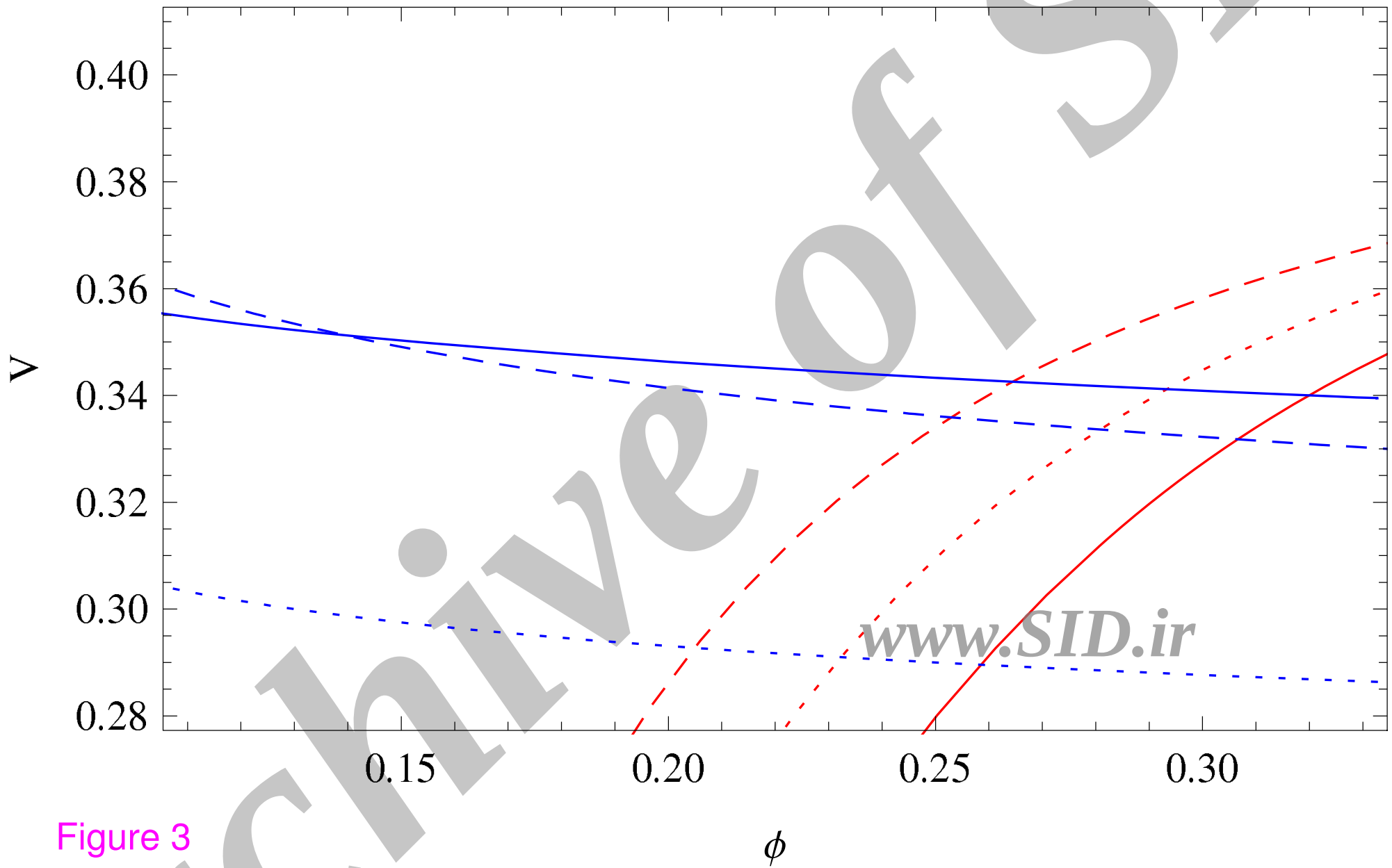

Figure 3

www.SID.ir

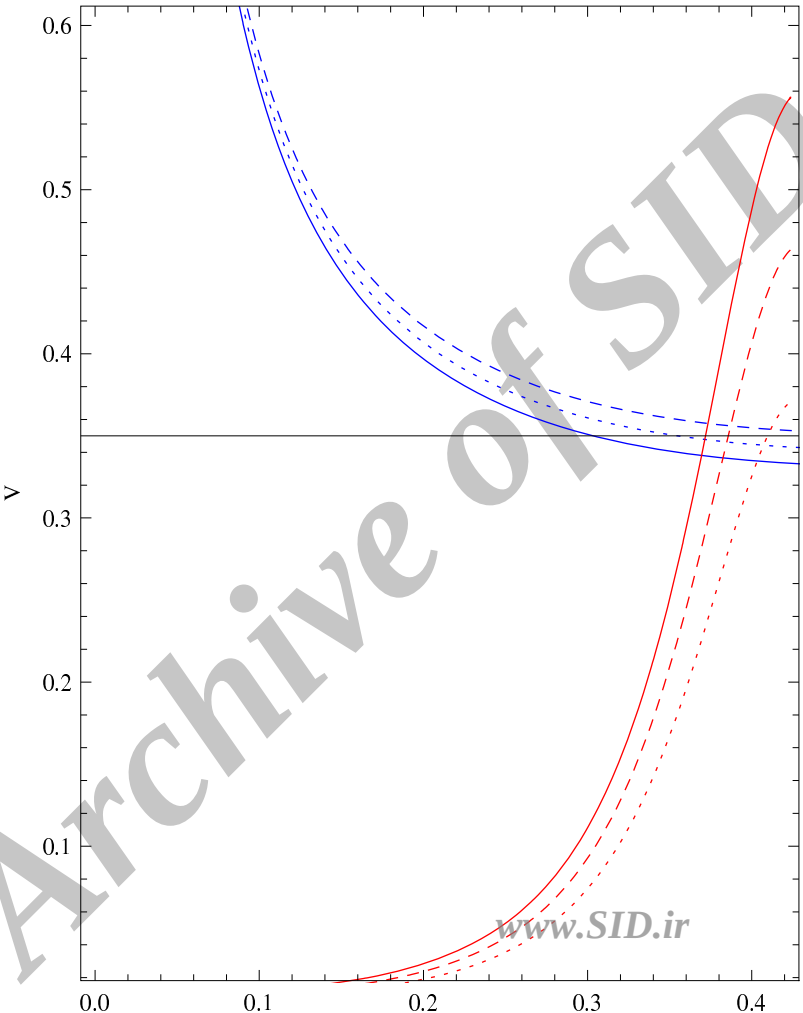

Figure 4

Archive of SID
www.SID.ir

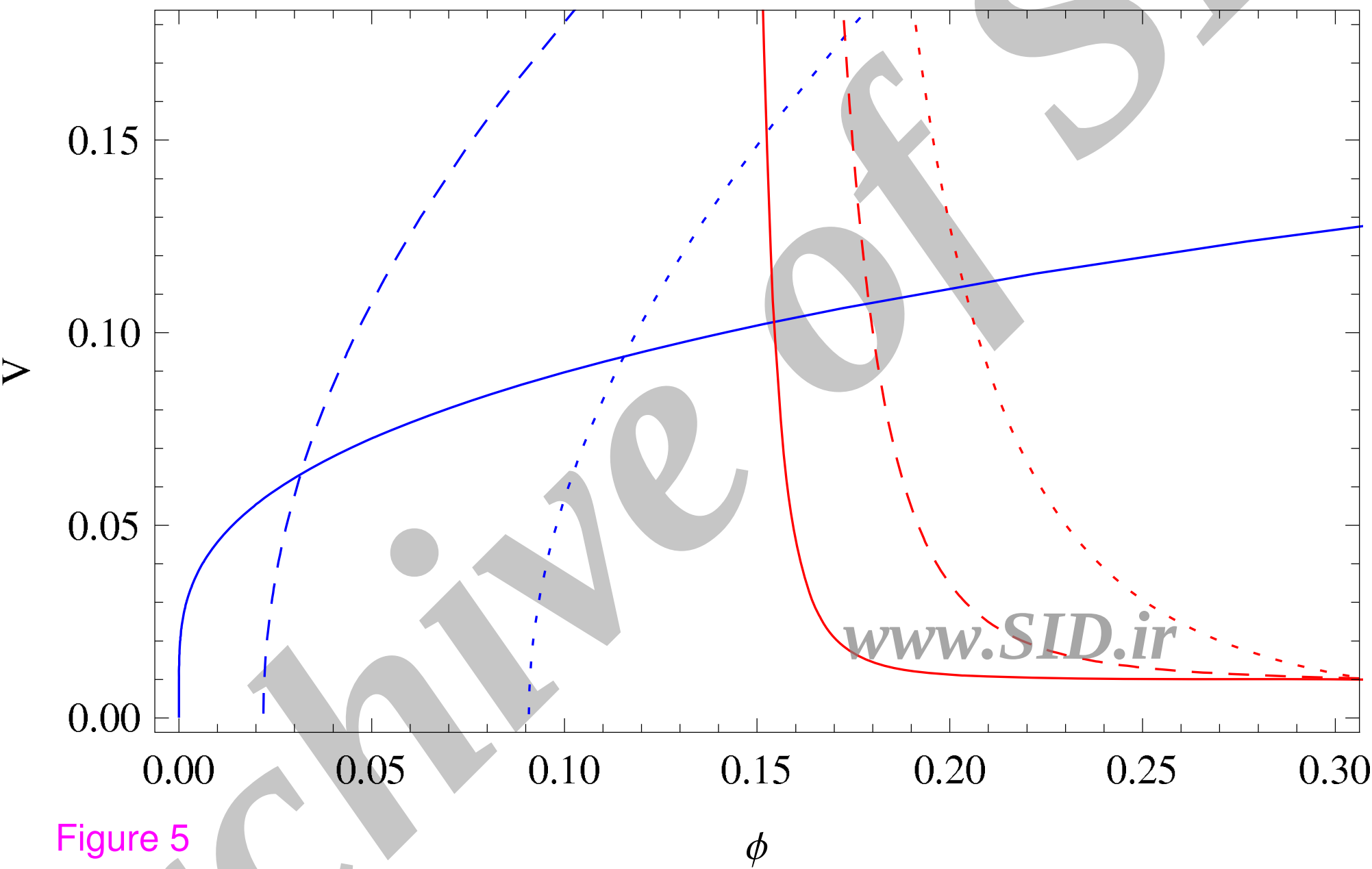

www.SID.ir

Figure 5

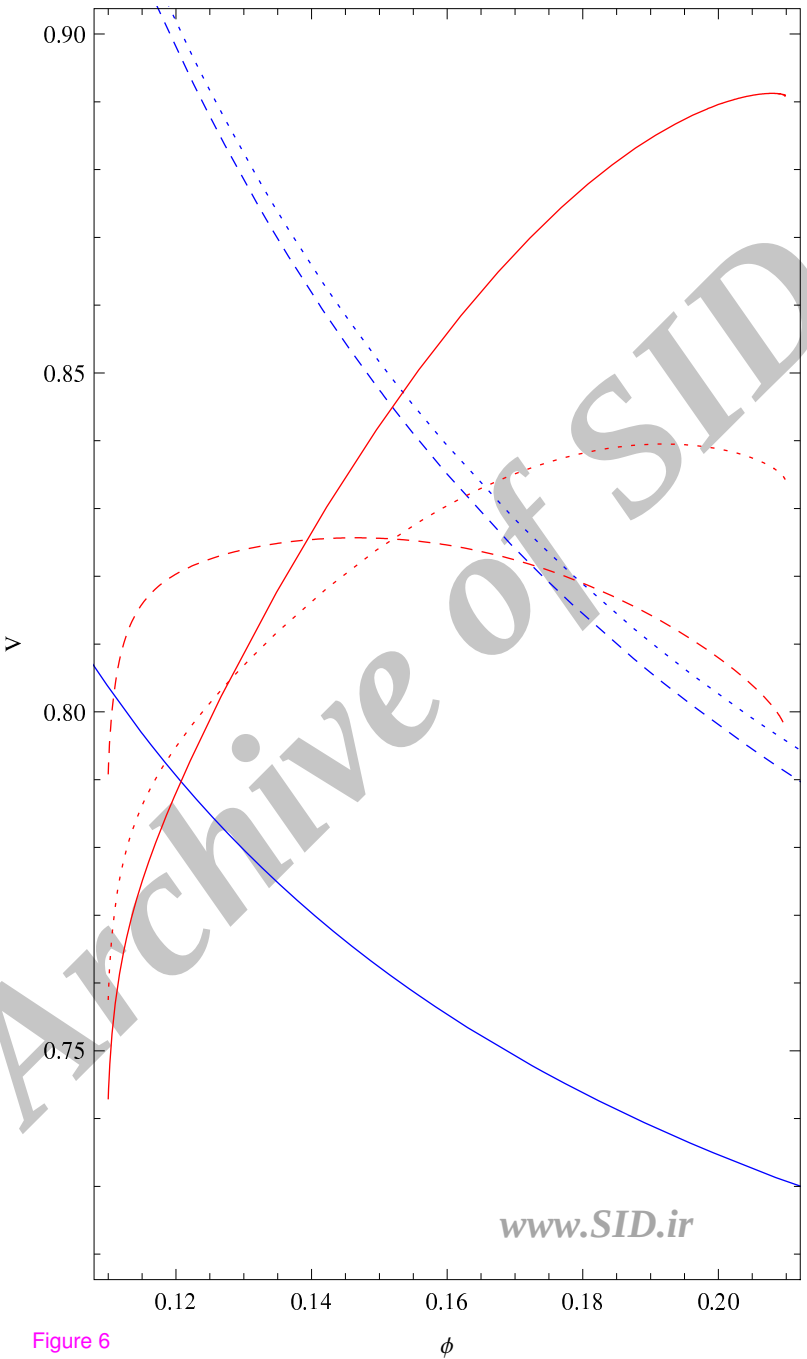

Archive of SID
www.SID.ir

Figure 6

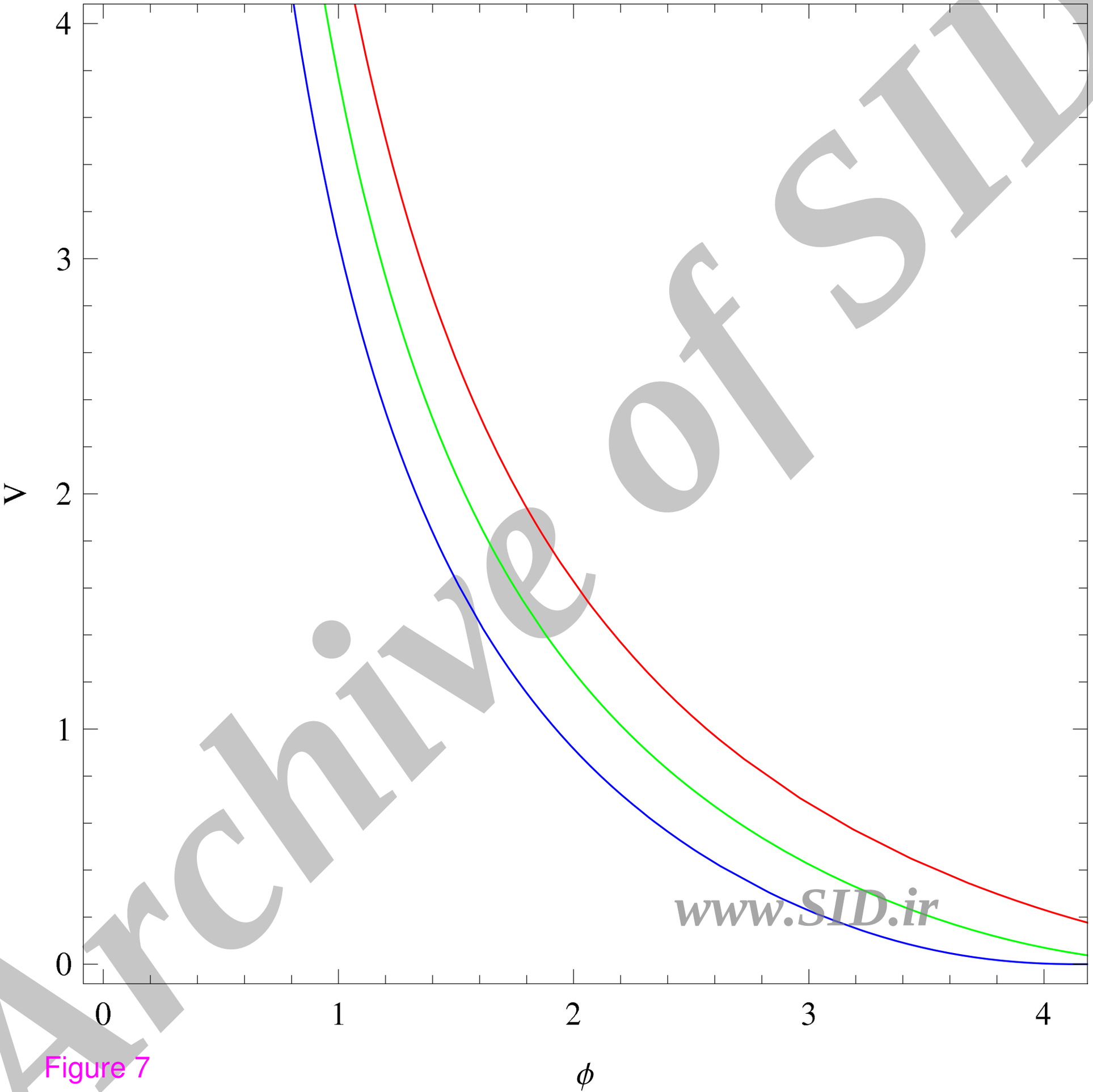

Archive of SID
www.SID.ir

Figure 7

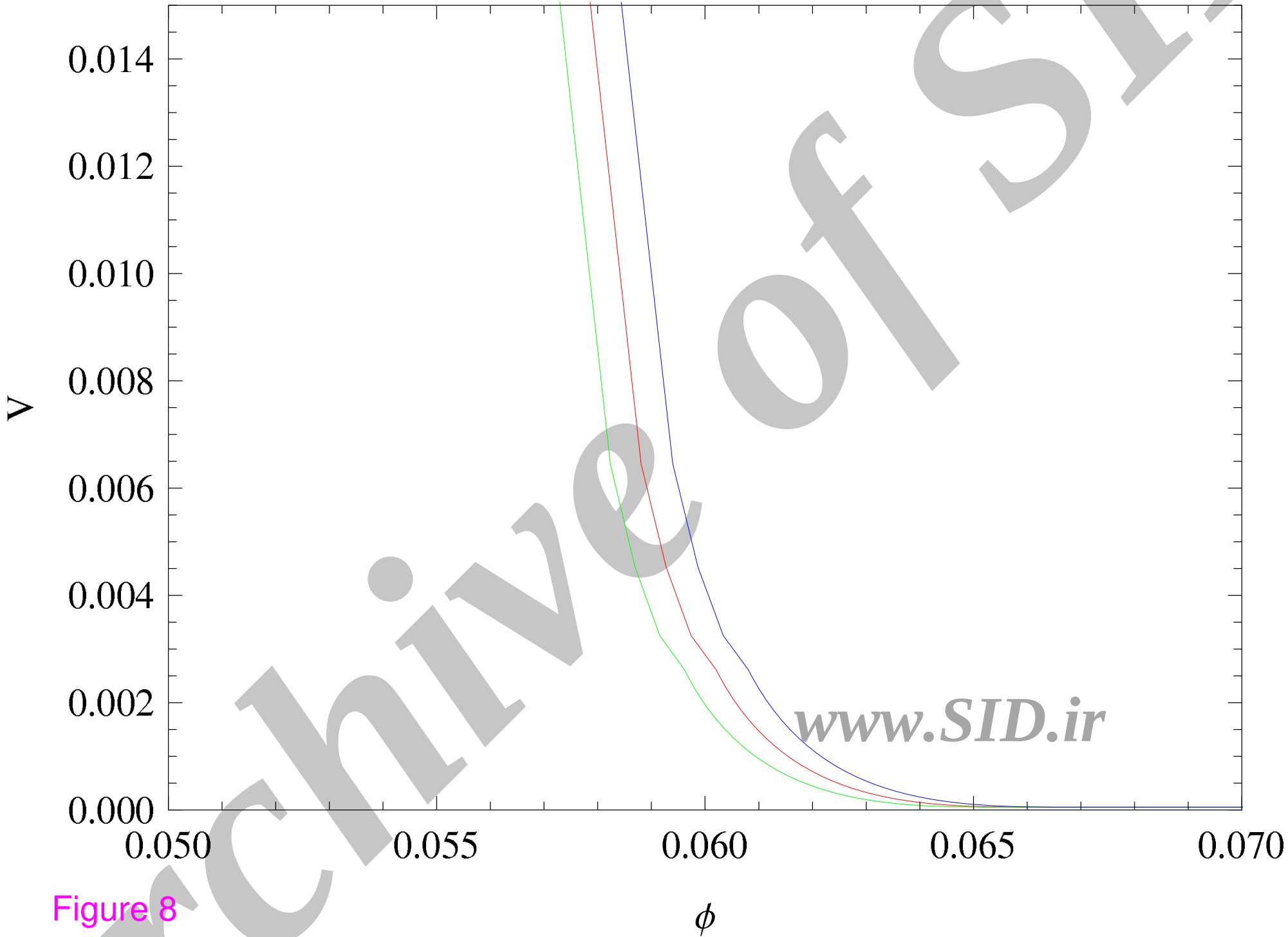

www.SID.ir

Figure 8

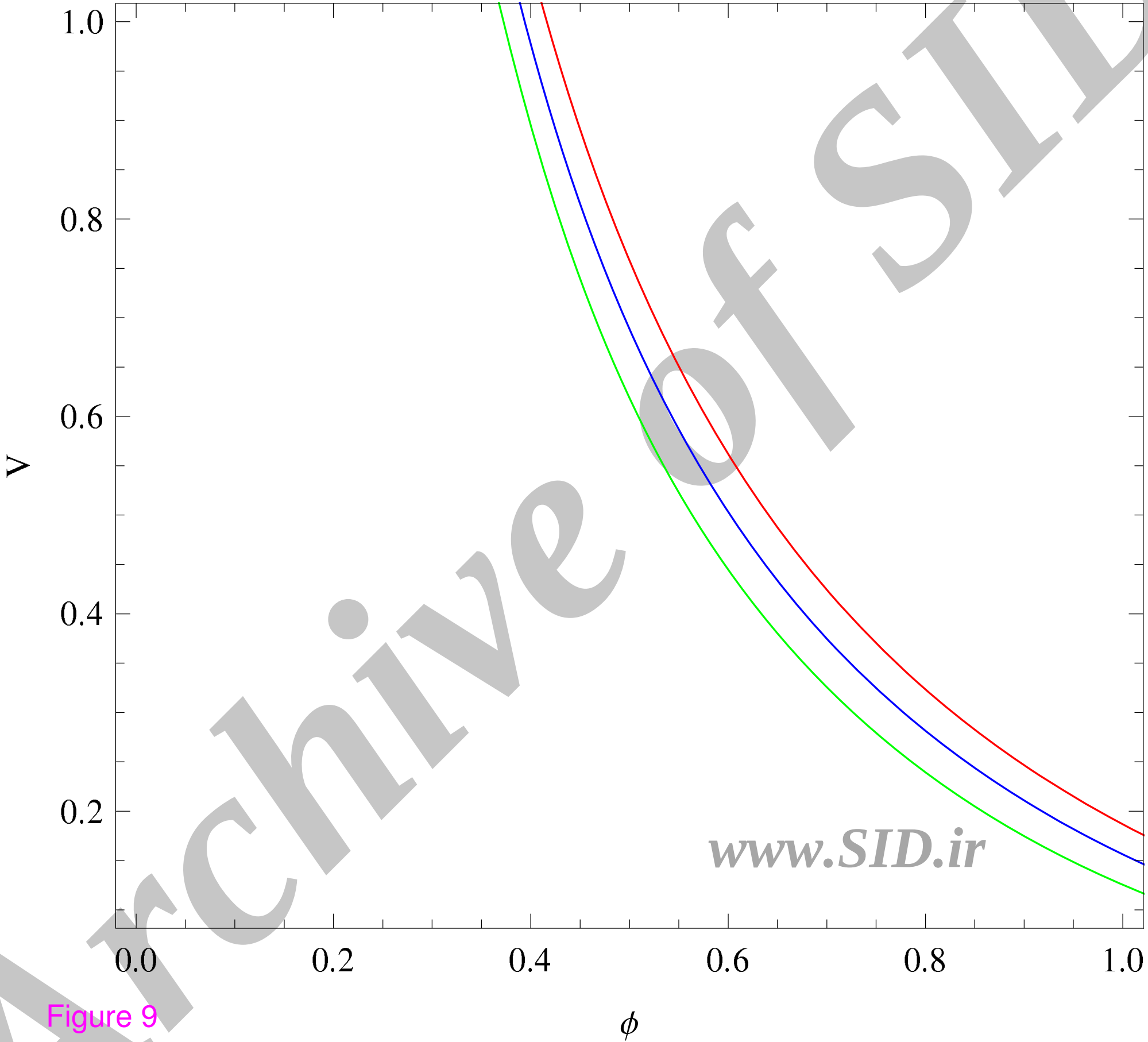

Archive of SID
www.SID.ir

Figure 9

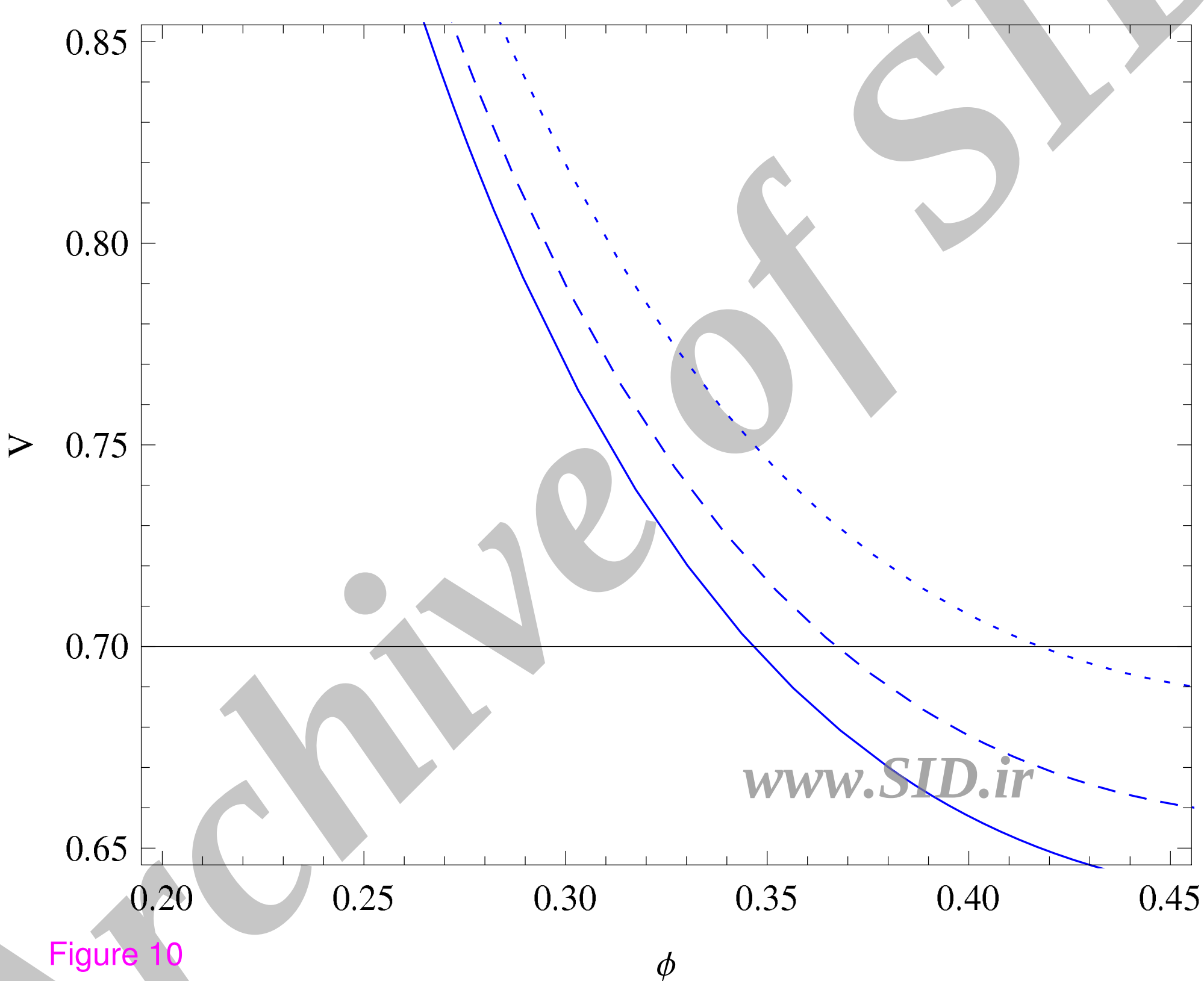

Archive of SID
www.SID.ir

Figure 10

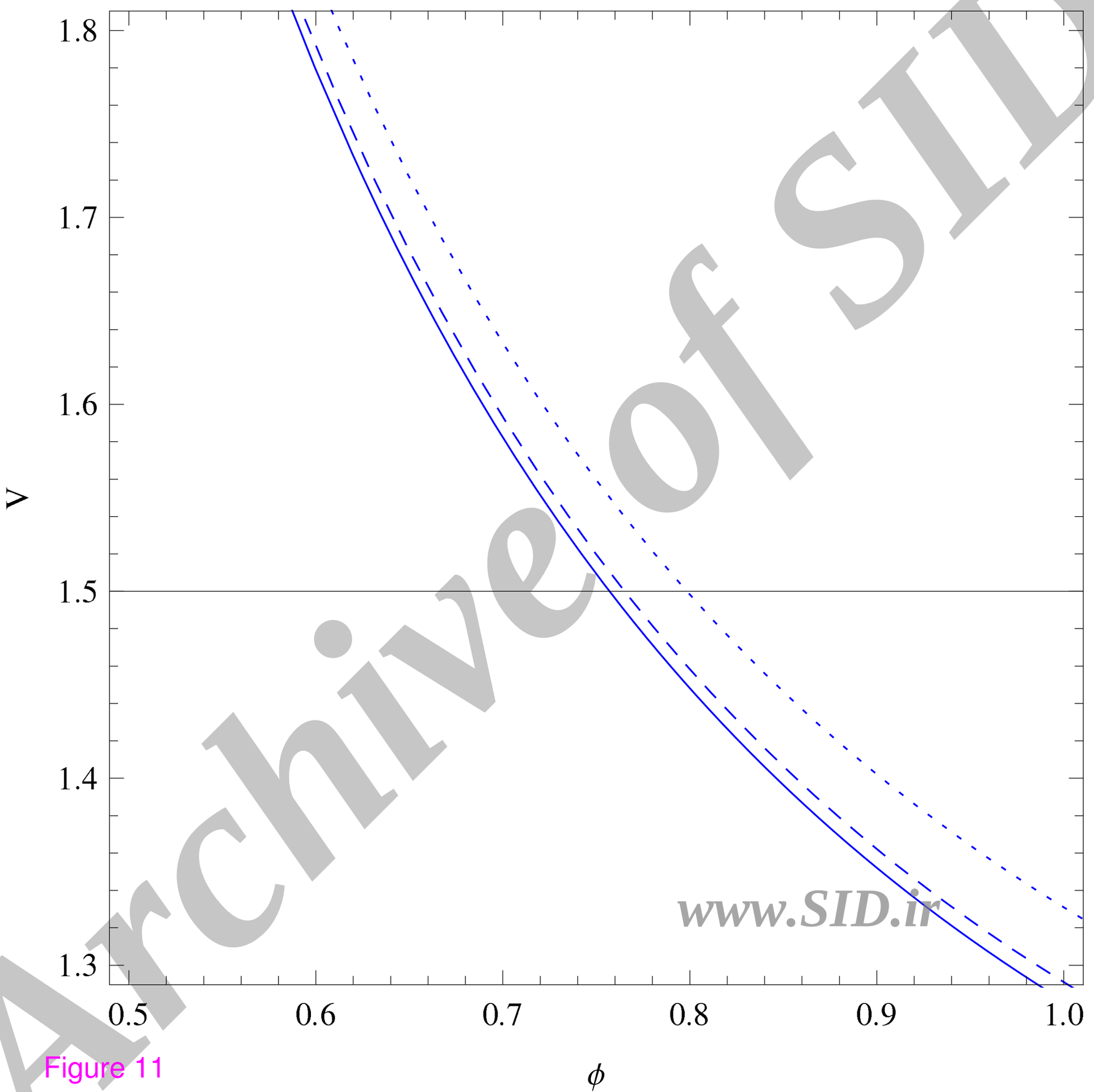

Archive of SID
www.SID.ir

Figure 11

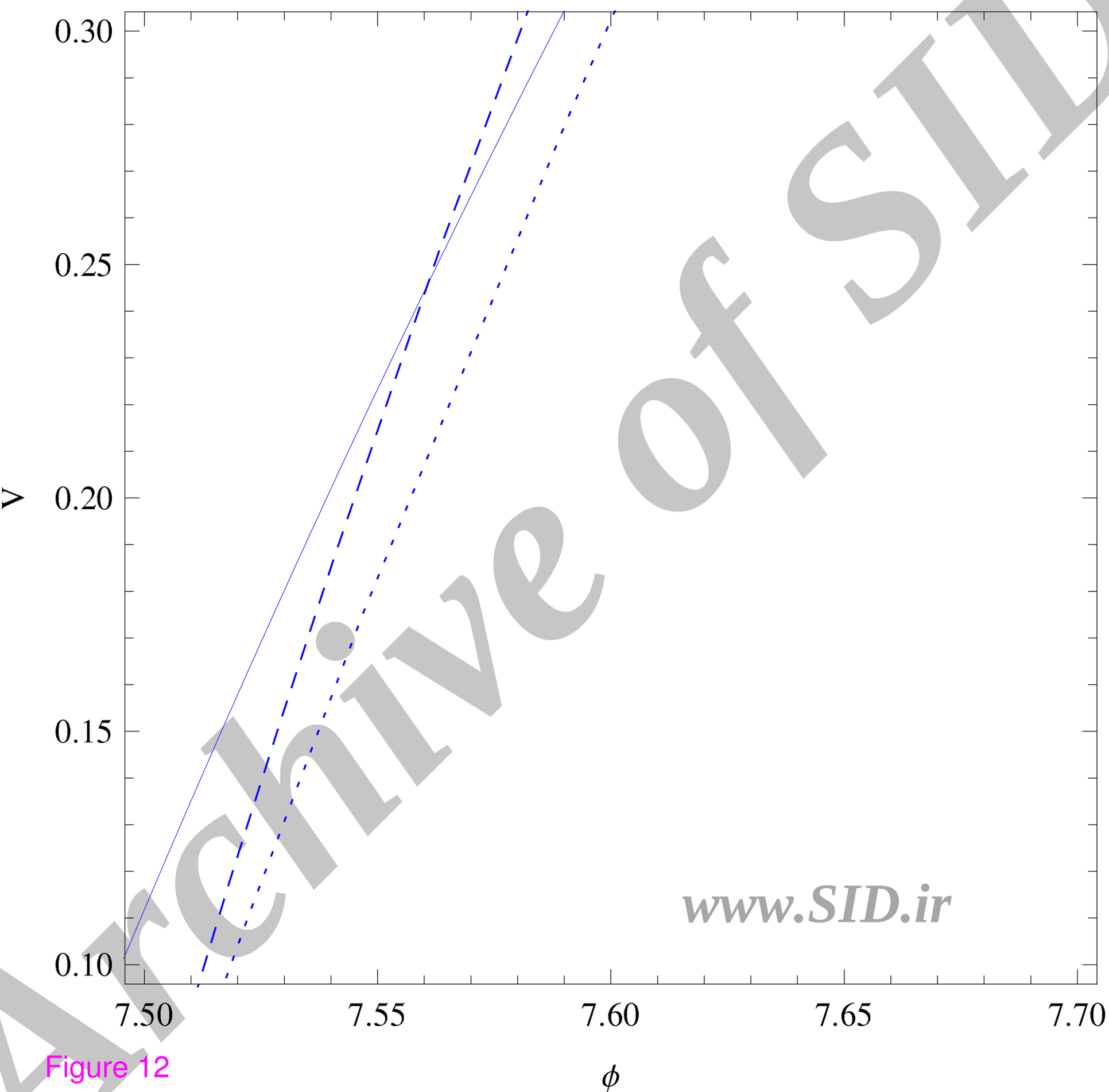

Archive of SID
www.SID.ir

Figure 12

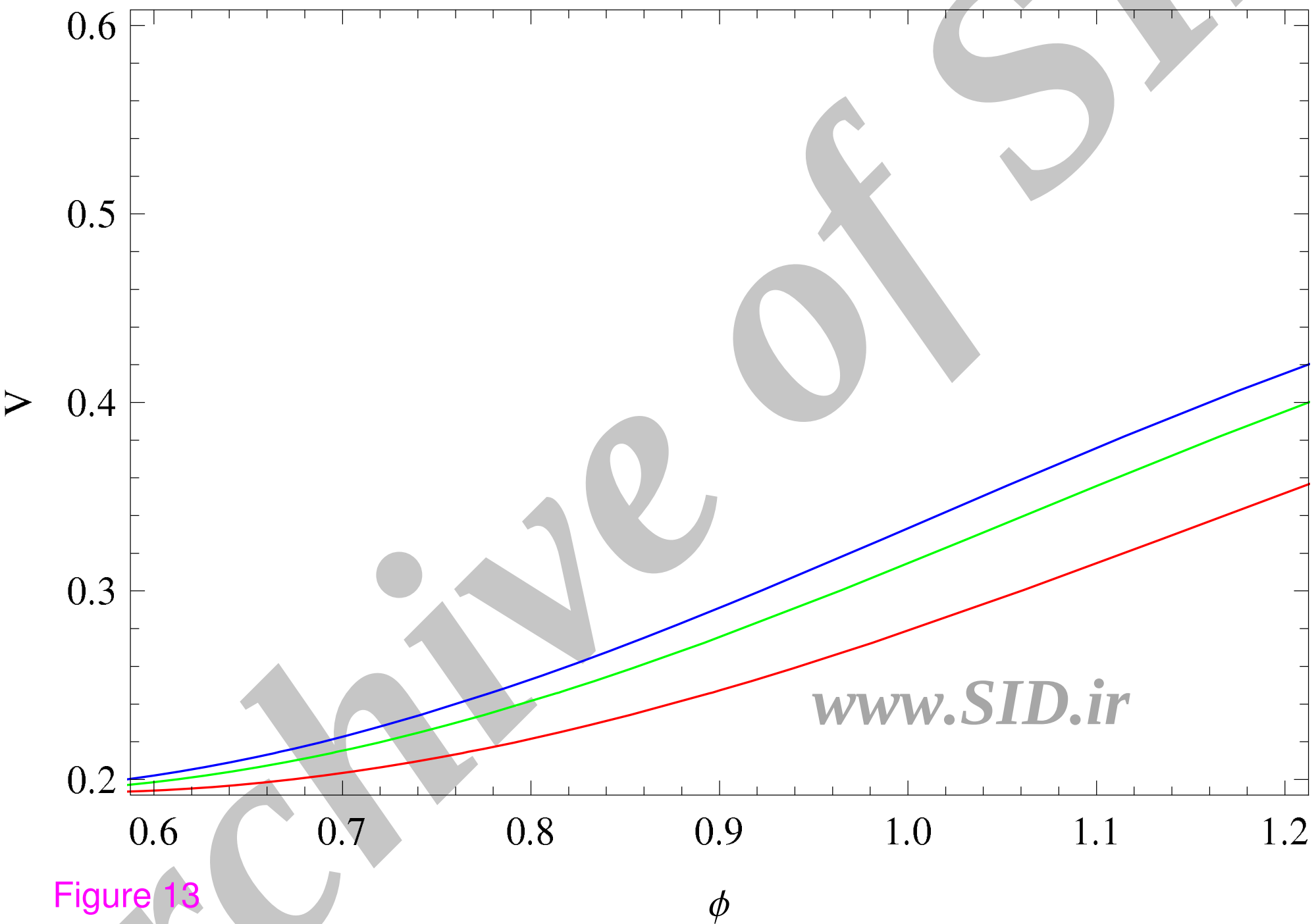

www.SID.ir

Figure 13

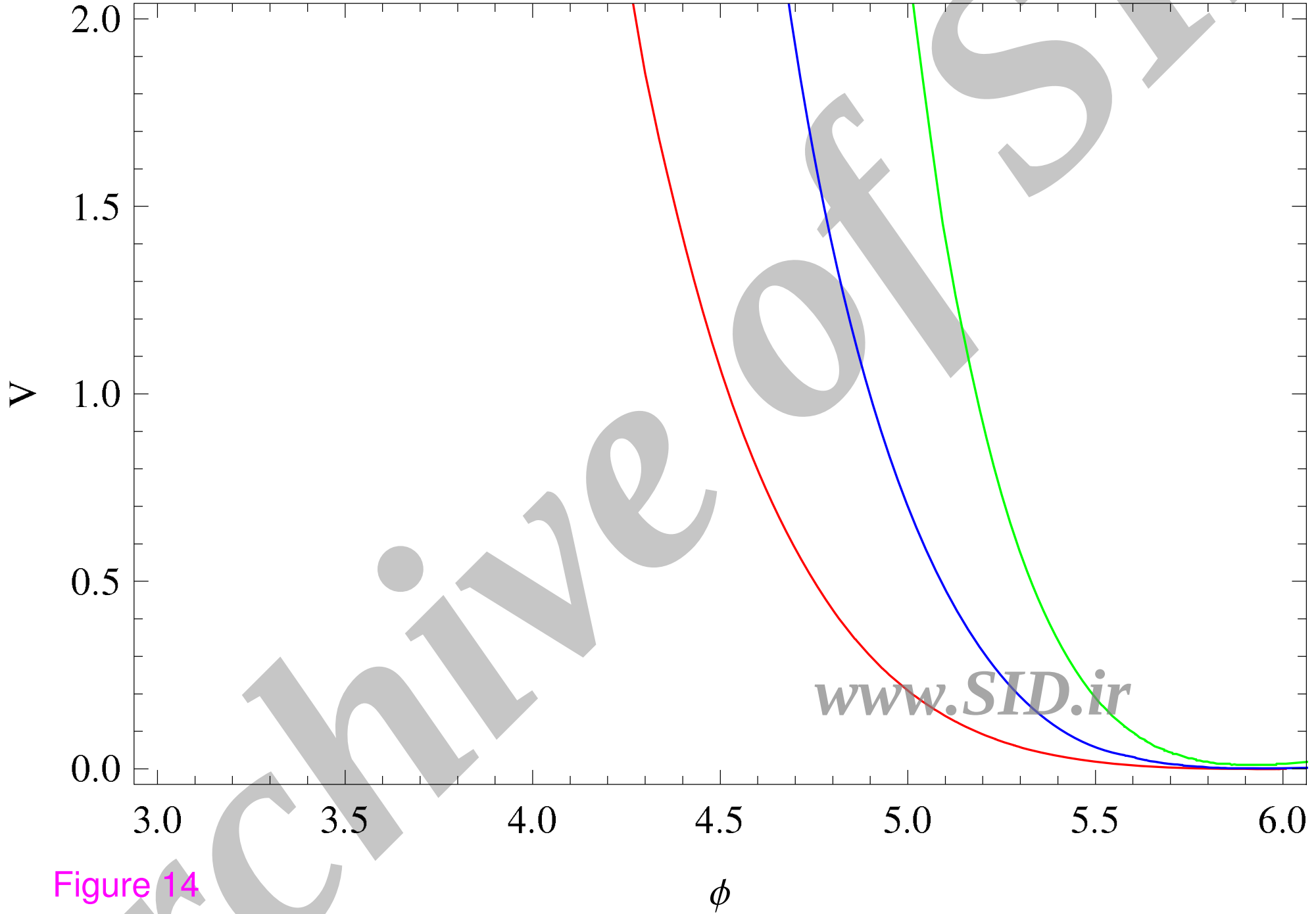

Figure 14

Archive of SID
www.SID.ir

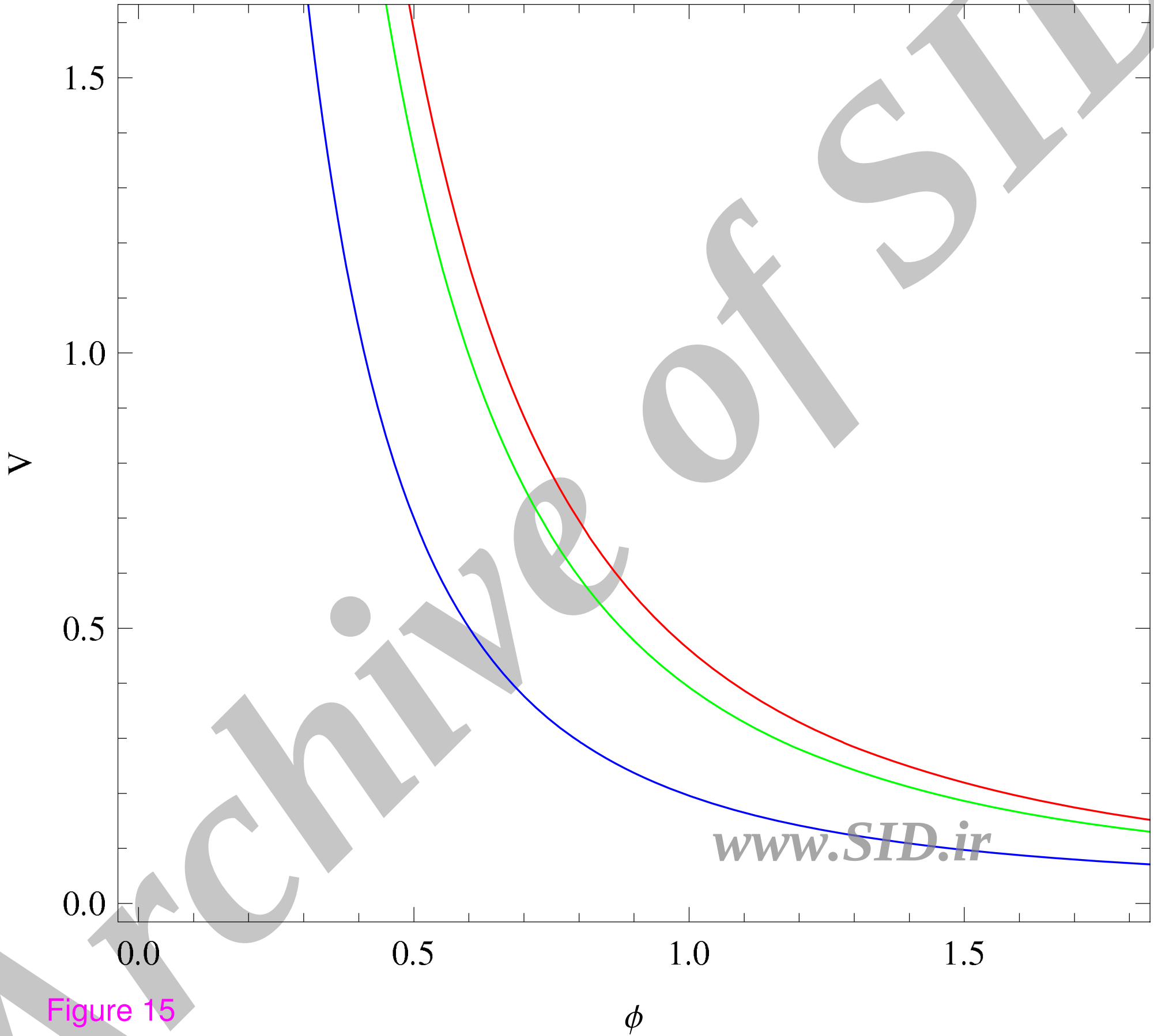

Archive of SID
www.SID.ir

Figure 15

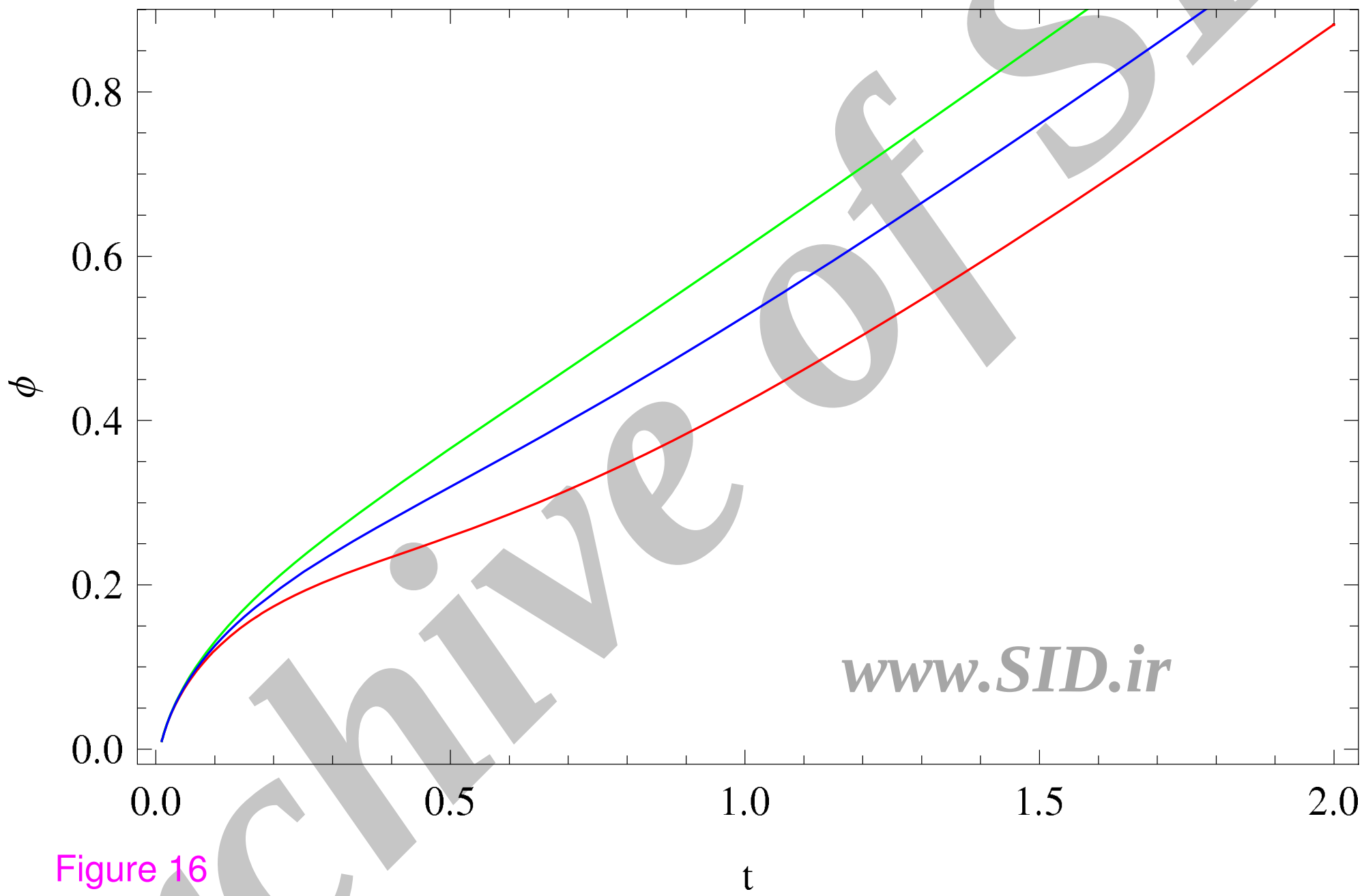

Figure 16

www.SID.ir

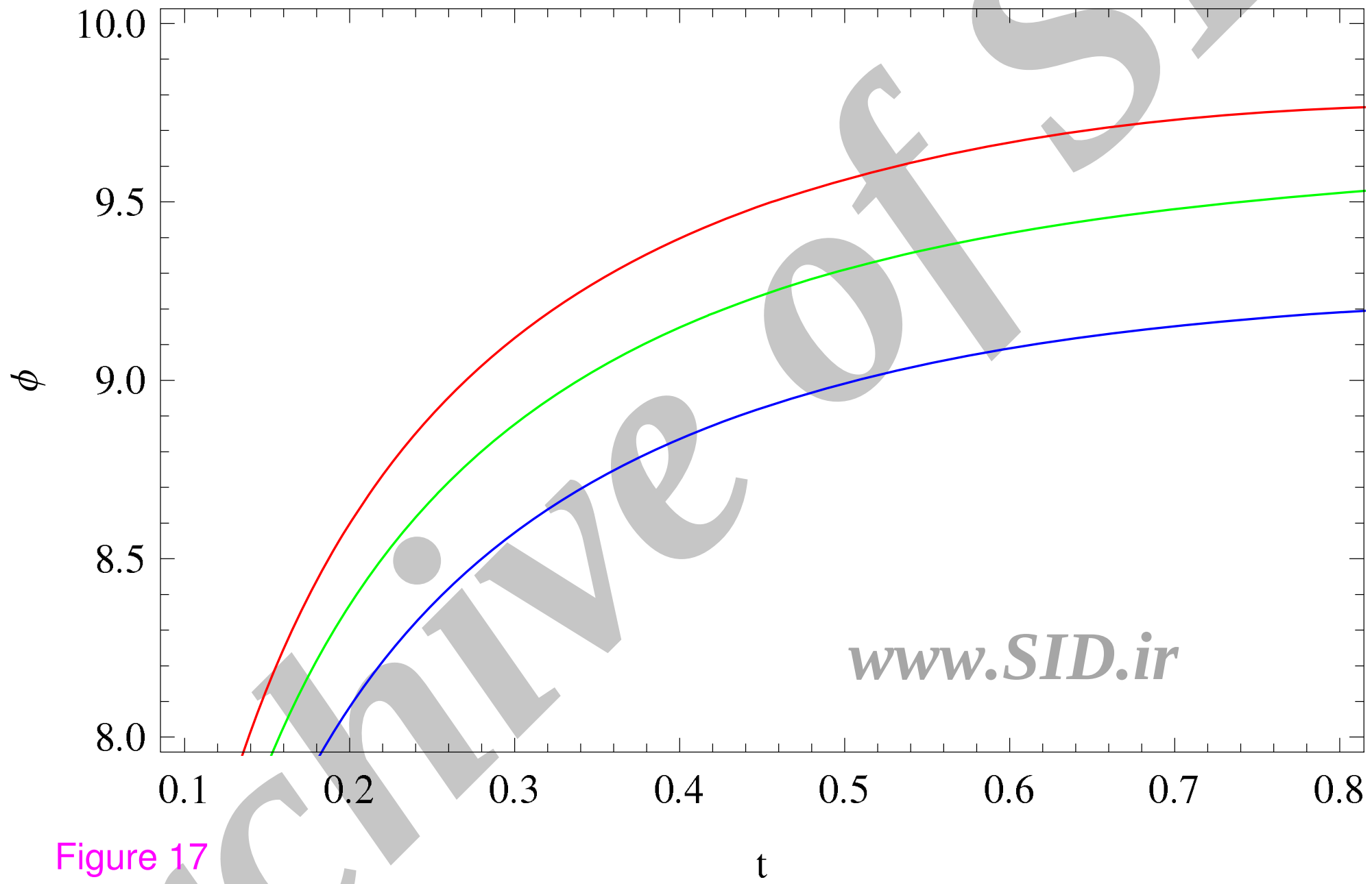

www.SID.ir

Figure 17

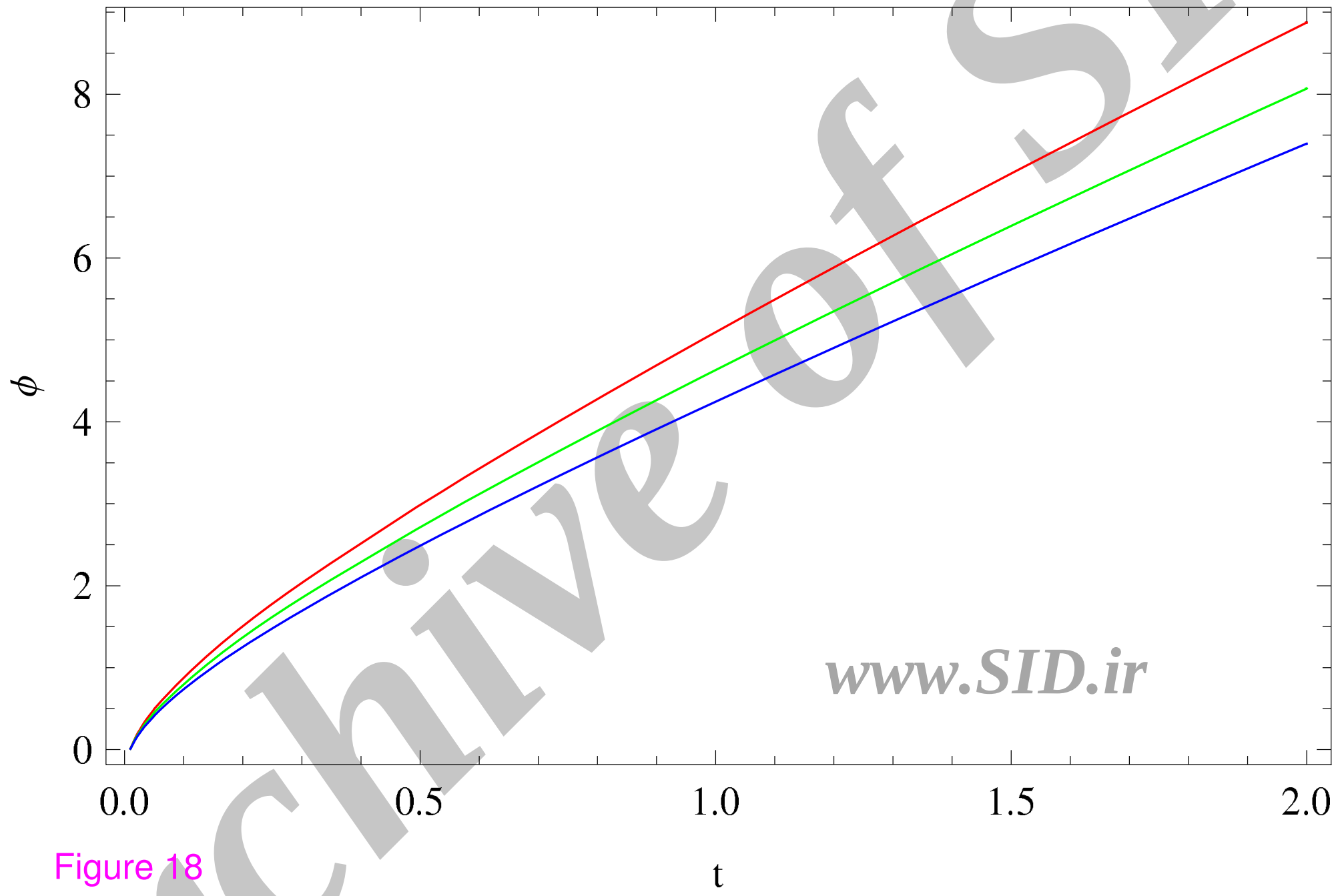

Figure 18

www.SID.ir

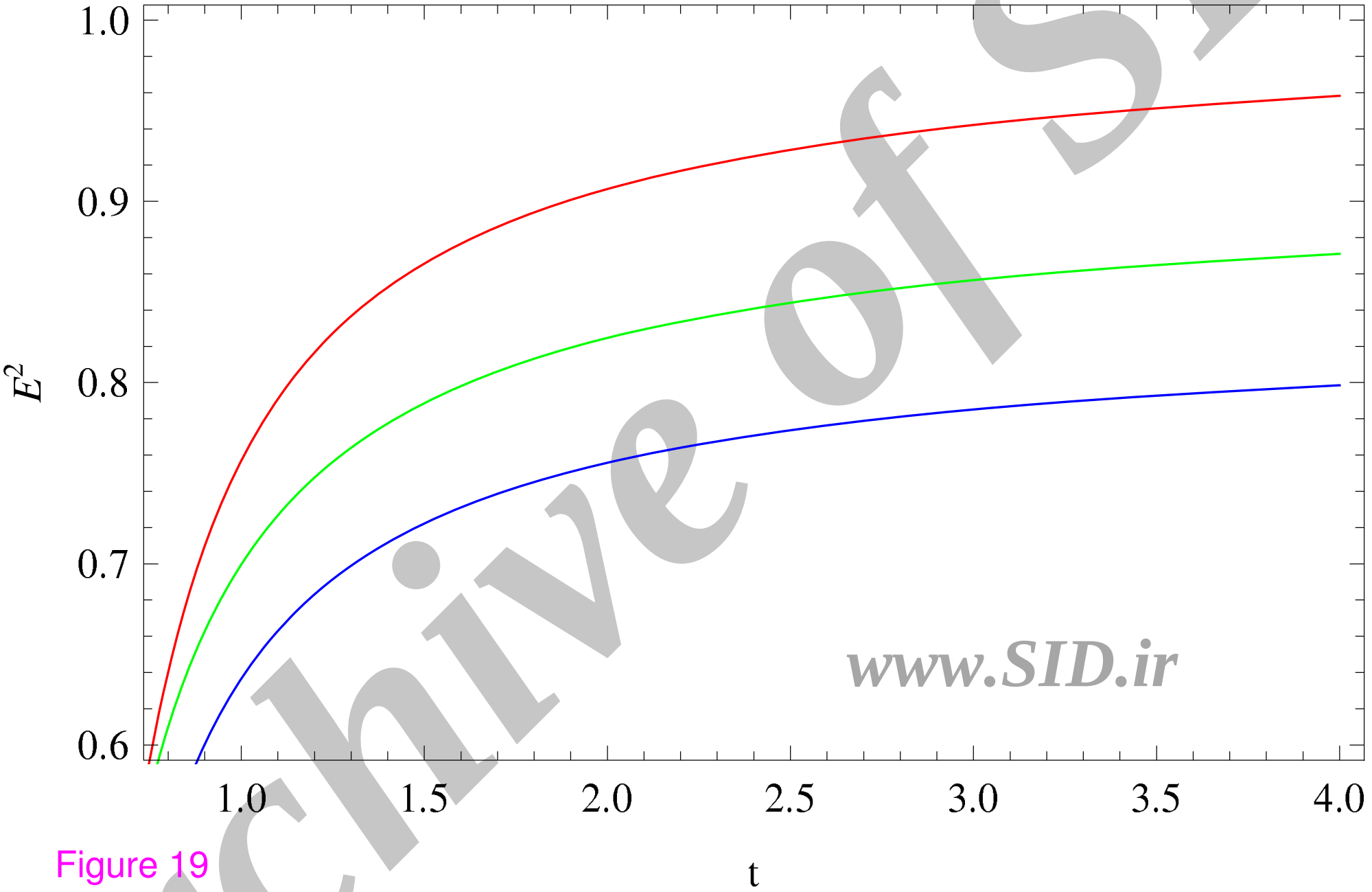

www.SID.ir

Figure 19

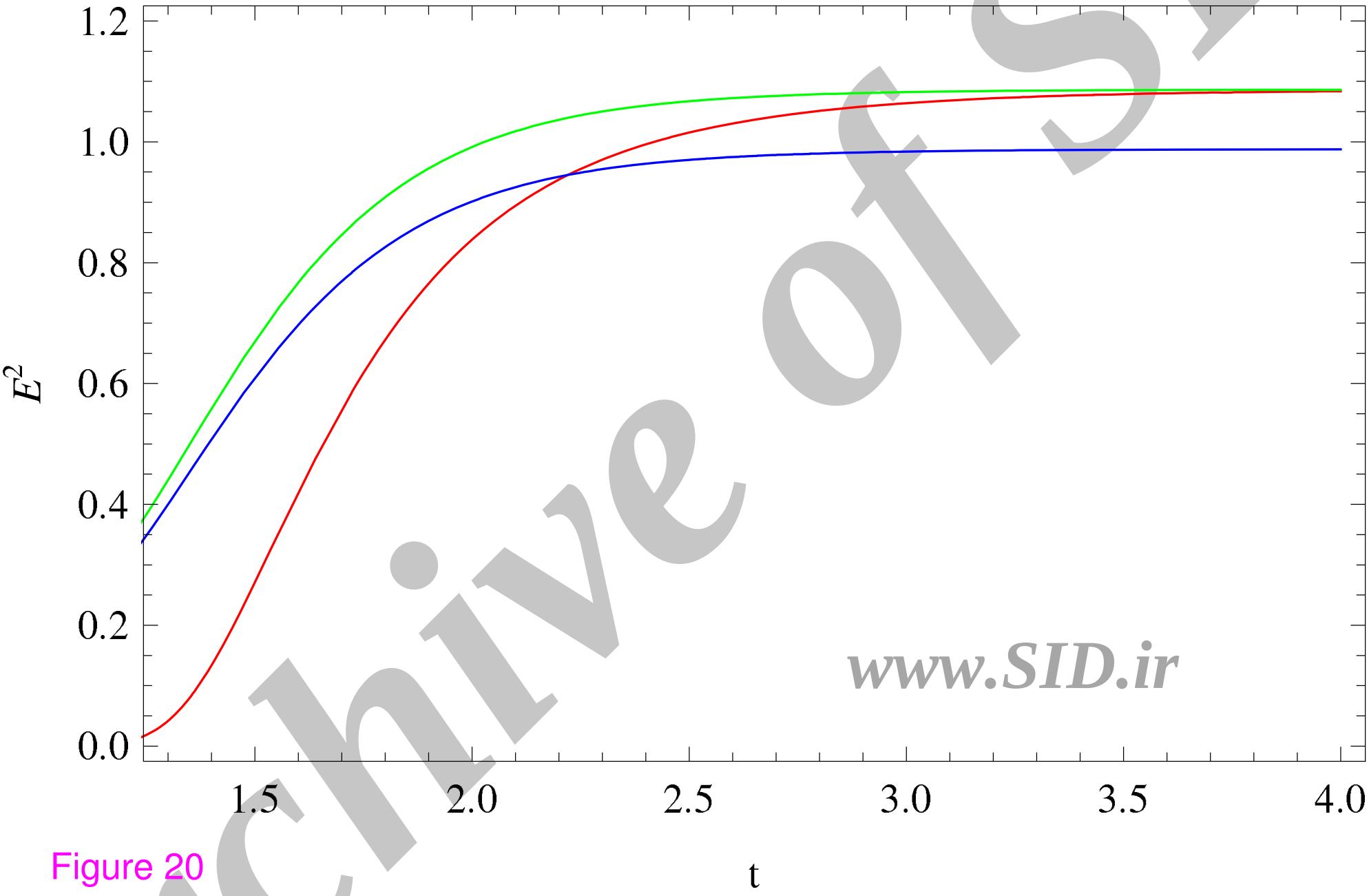

www.SID.ir

Figure 20

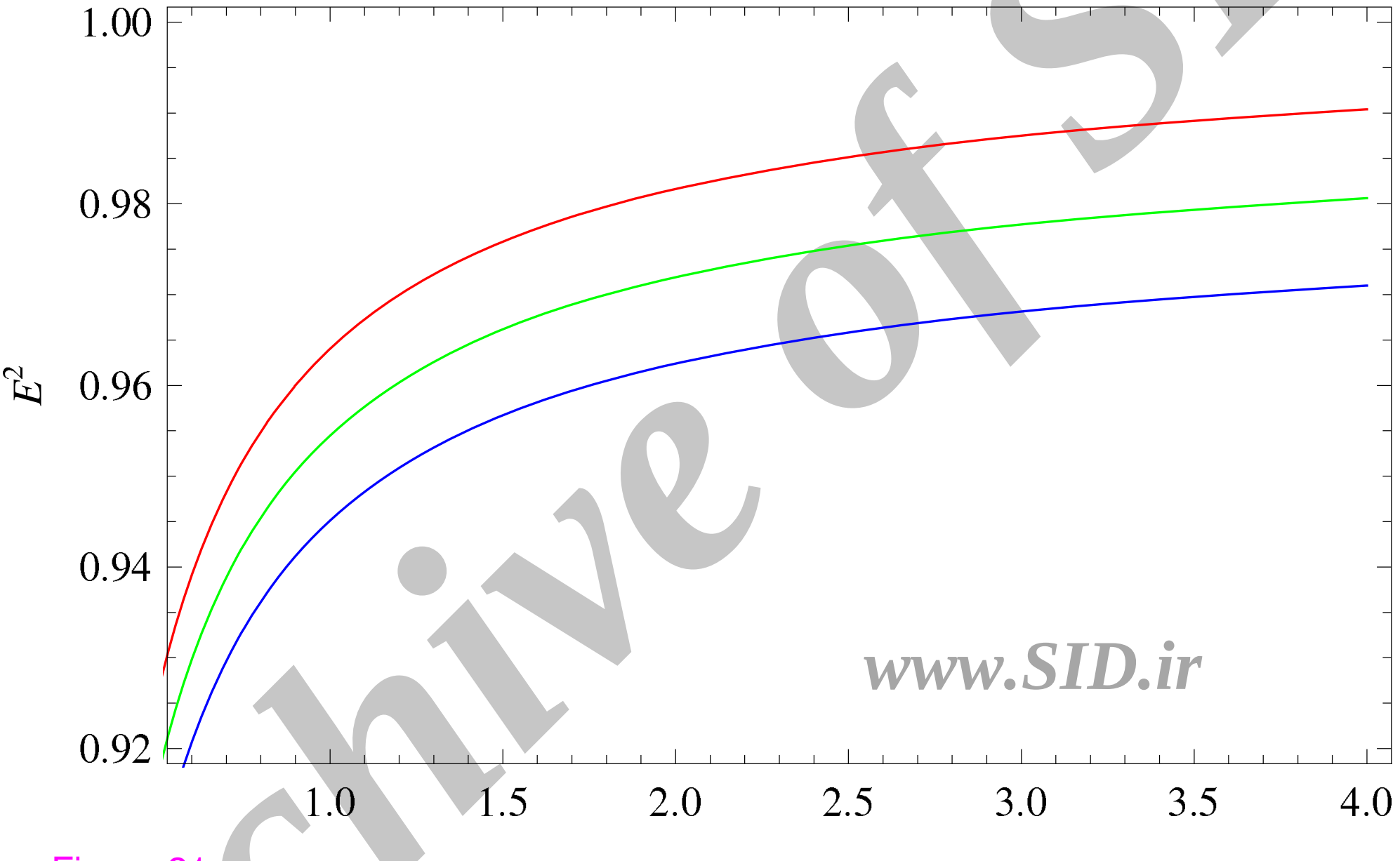

www.SID.ir

Figure 21